

**NASA Contractor Report 181928**

**ICASE Report No. 89-47**

# ICASE

## **NEAR-PLANAR TS WAVES AND LONGITUDINAL VORTICES IN CHANNEL FLOW: NONLINEAR INTERACTION AND FOCUSING**

**P. Hall**

**F. T. Smith**

(NASA-CR-181928) NEAR-PLANAR TS WAVES AND  
LONGITUDINAL VORTICES IN CHANNEL FLOW:  
NONLINEAR INTERACTION AND FOCUSING  
Report (ICASE) 37 p

CSCL 01A

63/02

NPO-11098

unclass  
0237050

**Contract No. NAS1-18605**

**September 1989**

**Institute for Computer Applications in Science and Engineering  
NASA Langley Research Center  
Hampton, Virginia 23665-5225**

**Operated by the Universities Space Research Association**



**National Aeronautics and  
Space Administration**

**Langley Research Center  
Hampton, Virginia 23665-5225**



**NEAR-PLANAR TS WAVES AND LONGITUDINAL  
VORTICES IN CHANNEL FLOW: NONLINEAR  
INTERACTION AND FOCUSING**

P. Hall<sup>1</sup>

Department of Mathematics  
University Exeter  
EX4 4QE, U.K.

F. T. Smith

Department of Mathematics  
University College London  
Gower Street, London WC1E 6BT, U.K.

**ABSTRACT**

The nonlinear interaction between planar or near-planar Tollmien-Schlichting waves and longitudinal vortices, induced or input, is considered theoretically for channel flows at high Reynolds numbers. Several kinds of nonlinear interaction, dependent on the input amplitudes and wavenumbers or on previously occurring interactions, are found and are inter-related. The first, Type a, is studied the most here and it usually produces spanwise focusing of both the wave and the vortex motion, within a finite scaled time, along with enhancement of both their amplitudes. This then points to the nonlinear interaction Type b where new interactive effects come into force to drive the wave and the vortex nonlinearly. Types c,d correspond to still higher amplitudes, with c being related to b, while d is connected with a larger-scale interaction e studied in an allied paper. Both c,d are subsets of the full three-dimensional triple-deck-like interaction, f. The strongest nonlinear interactions are those of d,e,f since they alter the mean-flow profile substantially, i.e., by an  $O(1)$  relative amount. All the types of nonlinear interaction however can result in the formation of focussed responses in the sense of spanwise concentrations and/or amplifications of vorticity and wave amplitude.

---

<sup>1</sup>This research was supported by the National Aeronautics and Space Administration under NASA Contract No. NAS1-18605 while the first and second author was in residence at the Institute for Computer Applications in Science and Engineering (ICASE), NASA Langley Research Center, Hampton, VA 23665.



## 1. INTRODUCTION

A fairly common feature in experiments and large-scale computations on channel-flow transition, as well as boundary-layer transition, with or without wall curvature, is the appearance quite early on of significant streamwise streaks following the spanwise concentration of streamwise vorticity. These streaks are possibly associated with the creation of Lambda vortices. Channel-flow experiments are described by Nishioka et al. (1975, 1980, 1985), Kozlov and Ramazanov (1982, 1983, 1984), Ramazanov (1985), among others, and related computations are by Kleiser et al. (1982, 1985), Orszag et al. (1980, 1983), Biringen et al. (1984), Zhou and Wang (1984), Zang and Hussaini (1985), Gilbert and Kleiser (1986), Singer et al. (1986), among others, under various disturbance conditions. It appears however that no rational or other theory has been put forward yet to account for the focusing of streamwise vorticity and the eventual formation of streaks. The present theoretical work is aimed at providing such an account, as well as enlarging the understanding of Tollmien-Schlichting/longitudinal-vortex interaction.

The theory is for an incompressible fluid in unsteady three-dimensional (3D) motion at high Reynolds numbers, starting with an initial input which is a near-2D Tollmien-Schlichting (TS) wave. A slight 3D “warping” present in the TS wave provokes a slight vortex motion as part of the mean-flow correction. This then poses a number of physical and theoretical questions. The first question to be addressed is how nonlinear interaction can take place between the evolution of the TS wave and that of the induced vortex flow, i.e., what structures are involved? The second question concerns whether the interaction is self-sustaining or instead peters out, and, third, how dependent is it on the initial input? Fourth, can theory predict the change of scale and spanwise focusing that seem central for the eventual description of streak formation?

These questions are considered in the following sections. In sections 2,3 it is found that the first occurrence (labelled Type a), or one of the first kinds, of such nonlinear interaction can arise for rather tiny amplitudes of the input TS wave<sup>3</sup> This tinyness is due essentially to the quite wide difference in the typical time scales for the viscous-inviscid TS wave and the induced vortex, which is initially viscous-controlled. The scales are derived from an order-of-magnitude argument in section 2, although they could be deduced instead from adaptation of the reasoning in Hall and Smith (1984, 1987). Next, the interaction turns out to be self-sustaining (section 4) in the sense that the slight warping of the 2DTS wave forces a very fast growth of the vortex motion which in turn reinforces the warping, and so on. At first this occurs in a form of linear secondary 3D instability which is different as a rule from

---

<sup>3</sup>Specifically, the TS streamwise velocity perturbation involved is of order  $Re^{-4/7}$ , suggesting a threshold of about 1% at Reynolds numbers  $Re$  in the range 1000-5000.

the suggested destabilization of Squire modes in that the secondary instability is found to be much more violent than previously suggested (although the subsequent interactions below do re-establish the importance of Squire-mode destabilization). After that, nonlinearity soon takes control and the indications, again from section 4, are that the nonlinear TS-vortex interaction terminates within a finite scaled time with the formation of concentrated zones or tongues of enhanced streamwise vorticity and TS amplitude (as well as phase variation), at particular spanwise locations. These vorticity tongues are felt to presage the initial development of a typical streak. A change of scale therefore takes place then, bringing in new physical properties associated with higher amplitudes inside the tongue, and this defines a second Type b of nonlinear interaction, as discussed in section 5. Further Types c,d,e are identified in section 6, along with the connections between the Types a-e. Throughout, the nonlinear behavior exhibits a sensitive dependence on the initial conditions; moreover, less civilized transitions than the experimental, computational and theoretical ones concerned above can by-pass any of the present regimes and enter later, higher-amplitude, stages directly. Further comments on these and other aspects are presented in section 7.

The velocities  $u, v, w$  and the corresponding cartesian coordinates  $x, y, z$  are based on nondimensionalization with respect to  $u_D$ , one-quarter of the maximum speed of the undisturbed plane Poiseuille flow, and to the channel width  $a_D$ , respectively. The undisturbed flow has  $u = \bar{u}(y) \equiv y - y^2$  (with  $v, w$  zero) between the walls  $y = 0, 1$ , properties at which are denoted by superscripts  $\mp$  in turn. The pressure is written  $\rho_D, u_D^2 p$  and the Reynolds number is  $\text{Re} = u_D a_D / \nu_D$ , where  $\rho_D, \nu_D$  are the density and kinematic viscosity of the fluid. Time is written  $a_D t / u_D$ , and the subscripts  $r, i$  stand respectively for the real and imaginary parts of a quantity. The theory is concentrated nominally near the lower branch of the neutral curve for large  $\text{Re}$ : it happens that the Reynolds numbers of concern in the transition experiments are also large, and previous theoretical studies indicate that the present kind of approach can have application at relatively low, even subcritical, Reynolds numbers.

## 2. THE SCALES, AND THE CORE FLOW, FOR TYPE A INTERACTIONS

Only slight warping of a 2D TS wave in the incoming 2D plane Poiseuille flow is necessary to provoke a nonlinear interaction between the wave and the longitudinal vortices created by the warping. The scales involved arrange themselves as follows for the first, Type a, interaction to be considered here: see also Figure 1. First of all, the typical time or length scales of the primary TS wave and a longitudinal vortex are very different, the time scales being  $0(\varepsilon^{-3})$  and  $0(\varepsilon^{-7})$  in turn, where  $\varepsilon \equiv \text{Re}^{-1/7}$  is small. The former size comes straight from properties of the Orr-Sommerfeld equation at large  $\text{Re}$  and helps fix the thin viscous critical-layer/wall-layer width, while the induced longitudinal vortex in the core responds

initially at least with an unsteady-viscous force balance, so that  $\partial_t \sim \text{Re}^{-1}$ . This relative discrepancy of order  $\varepsilon^4$  in the time scales or  $\varepsilon^6$  in the lengths implies that a crucial amplitude of the 2D TS wave is of order  $\varepsilon^3$ , in relative terms, since the critical nonlinear interplay is expected to be due to amplitude-squared inertial effects acting on the  $x$ -scale  $0(\varepsilon^{-1})$  characteristic of a 2D TS wave, and that determines the TS disturbance amplitude in the core ( $0 < y < 1$ ) and the wall layers ( $y \approx 0, 1$ ) examined below. A similar reasoning based on physical balances also points to the slow  $z$ -scale of interest, namely  $z \sim \varepsilon^{-3}$ , for the spanwise warping in the TS wave to be significant, as opposed to the main  $x$ -scale of  $0(\varepsilon^{-1})$ . Likewise, the induced vortex amplitude follows as  $0(\varepsilon^4)$ , in the velocity  $u$ , because of its production by means of amplitude-squared effects from the TS disturbance, in the core of the flow. So multiple scaling is called for, in the form

$$\partial_x \rightarrow \varepsilon \partial_X, \quad \partial_z \rightarrow \varepsilon^3 \partial_Z, \quad \partial_t \rightarrow \varepsilon^3 \partial_T + \varepsilon^7 \partial_{\bar{T}} \quad (2.1)$$

where  $x = \varepsilon^{-1}X$ ,  $z = \varepsilon^{-3}Z$ ,  $t = \varepsilon^{-3}T$ ,  $t = \varepsilon^{-7}\bar{T}$ , and so on, along with the core- and wall-layer expansions set out just below and in the next section. A noteworthy feature in both cases is the fairly tiny size, in both the TS and the vortex disturbances, at which nonlinear interaction first enters; this tinyness seems to stem originally from their disparity in characteristic time scales and it seems to tie in with some experimental observations.

In the core of the undisturbed motion, the flow solutions for the velocity and pressure take the form

$$u = \bar{u}(y) + \varepsilon^4 u^{(3)} + \varepsilon^5 u^{(1)} + \varepsilon^7 u^{(e)} + \dots + \varepsilon^9 u^{(f)} + \dots \quad (2.2a)$$

$$v = \varepsilon^6 v^{(1)} + \varepsilon^8 v^{(e)} + \dots + \varepsilon^{10} v^{(f)} + \dots + \varepsilon^{11} v^{(3)} + \dots \quad (2.2b)$$

$$w = \varepsilon^8 w^{(3)} + \varepsilon^9 w^{(1)} + \varepsilon^{11} w^{(e)} + \dots + \varepsilon^{13} w^{(f)} + \dots \quad (2.2c)$$

$$p = -k_o \varepsilon^6 X + \varepsilon^7 p^{(1)} + \varepsilon^9 p^{(e)} + \dots + \varepsilon^{11} p^{(f)} + \varepsilon^{12} p^{(3)} + \dots \quad (2.2d)$$

where the superscript (3) refers to the induced vortex flow which is dependent on  $\bar{T}, Z, y$  but independent of the fast scales  $X, T$ , while (1) refers to the nonlinear TS wave (dependent on  $X, T, \bar{T}, Z, y$ ) and (e), (f) denote higher-order TS effects. Also, the constant  $k_o = 2$  from the basic flow. Substitution of (2.1), (2.2) into the continuity and Navier-Stokes equations then leads to the following successive balances controlling the TS wave and the longitudinal vortex in the core.

The TS wave at leading order satisfies, for continuity and the  $x$ -,  $y$ -,  $z$ - momentum balances in turn,

$$u_{X^{(1)}} + v_{y^{(1)}} = 0, \quad \bar{u}u_{X^{(1)}} + v^{(1)}\bar{u}' = 0, \quad (2.3a, b)$$

$$\bar{u}v_{X^{(1)}} = -p_{y^{(1)}}, \quad \bar{u}w_{X^{(1)}} = -p_{Z^{(1)}}, \quad (2.3c, d)$$

where the prime denotes  $d/dy$ . The solution here is neutral at this level of working, so that

$$\{u^{(1)}, v^{(1)}, w^{(1)}, p^{(1)}\} = \{A\bar{u}', -i\alpha A\bar{u}, \hat{p}^{(1)}, \hat{w}^{(1)}\}E + c.c. \quad (2.4)$$

where  $\hat{p}^{(1)}, \hat{w}^{(1)}$  are independent of  $X, T$ , the function  $A$  is independent of  $X, y, T$  and represents a negative displacement effect,

$$E \equiv \exp[i(\alpha X - \Omega T)] \quad (2.5)$$

with the wavenumber  $\alpha$  and the frequency  $\Omega$  both being real, and (2.3a-c) are satisfied provided that

$$\hat{p}^{(1)} = \hat{P}^{(1)-} - \alpha^A \int_0^y \bar{u}^2 dy, \quad \hat{w}^{(1)} = -\hat{p}_{Z(1)}/i\alpha\bar{u}. \quad (2.6a, b)$$

Here  $\hat{P}^{(1)-}(X, T, \bar{T}, Z, \dots)$  represents the lower-wall pressure, and the scaled pressure difference between the walls,

$$\hat{P}^{(1)+} - \hat{P}^{(1)-} = -\alpha^2 AI \quad [\text{where } I = 1/30], \quad (2.7)$$

is due to the curvature in the disturbed core flow and is a vital part of the nearly 2D TS wave. Also, ‘‘c.c.’’ denotes the complex conjugate of the preceding expression.

Next, the TS corrections  $u^{(e)}, \dots$  are governed by

$$u_{X^{(e)}} + v_{y^{(e)}} = 0, \quad u_{T^{(1)}} + \bar{u}u_{X^{(e)}} + v^{(e)}\bar{u}' = -p_{X^{(1)}}, \quad (2.8a, b)$$

$$v_{T^{(1)}} + \bar{u}v_{X^{(e)}} = -p_{y^{(e)}}, \quad w_{T^{(1)}} + \bar{u}w_{X^{(e)}} = -p_{Z^{(e)}}, \quad (2.8c, d)$$

thus bringing in the unsteadiness and streamwise pressure gradient of the TS wave. A decomposition as in (2.4),

$$\{u^{(e)}, v^{(e)}, w^{(e)}, p^{(e)}\} = \{\hat{u}^{(e)}, \hat{v}^{(e)}, \hat{w}^{(e)}, \hat{p}^{(e)}\}E + c.c. \quad (2.9)$$

therefore gives the results

$$\hat{u}^{(e)} = A^{(e)}\bar{u}' - \bar{u} \int \hat{p}^{(1)}\bar{u}^{-2} dy - \hat{p}^{(1)}/\bar{u}, \quad (2.10a)$$

$$\hat{v}^{(e)} = i\alpha\bar{u} \int \hat{p}^{(1)}\bar{u}^{-2} dy + i\Omega A - i\alpha A^{(e)}\bar{u}, \quad (2.10b)$$

$$\hat{p}_{y^{(e)}} = 2\alpha\Omega A\bar{u} + \alpha^2\bar{u}^2 \{-A^{(e)} + \int \hat{p}^{(1)}\bar{u}^{-2} dy\} \quad (2.10c)$$

where  $-A^{(e)}$  is an extra displacement effect.

Then the extra TS contributions  $u^{(f)}, \dots$  are the first ones to feel the influence of the unknown induced vortex flow  $[u^{(3)}, \dots]$  directly, through the governing equations

$$u_{X^{(f)}} + v_{y^{(f)}} = 0, \quad u_{T^{(e)}} + \bar{u}u_{X^{(f)}} + u^{(3)}u_{X^{(1)}} + v^{(f)}\bar{u}' + v^{(1)}u_{y^{(3)}} = -p_{X^{(e)}} \quad (2.11a, b)$$



$$v_{T^{(e)}} + \bar{u}v_{X^{(f)}} + u^{(3)}v_{X^{(1)}} = -p_{y^{(f)}}, w_{T^{(e)}} + \bar{u}w_{X^{(f)}} + u^{(3)}w_{X^{(1)}} + v^{(1)}w_y^{(3)} = -p_{Z^{(f)}} \quad (2.11c, d)$$

and the nonlinear inertial interaction between (1) and (3) terms. We note that any terms between  $u^{(e)}, u^{(f)}$  in (2.2a) and so on do not affect the present vortex/TS interaction. With the decomposition  $u^{(f)} = \hat{u}^{(f)}E + \text{c.c.}$ , etc., as in (2.4), (2.9), the solution here gives

$$\hat{v}^{(f)} = -i\alpha\{A^{(f)}\bar{u} + Au^{(3)} + A\Gamma^{(f)}(y)\}, \quad (2.12a)$$

$$\hat{p}^{(f)} = \hat{P}^{(f)-} - \alpha^2\{A^{(f)}\int_0^y \bar{u}^2 dy + 2A\int_0^y \bar{u}u_3 dy\} + A\gamma^{(f)}(y) \quad (2.12b)$$

where the functions  $\Gamma^{(f)}, \gamma^{(f)}$  are standard functions in the linear-stability expansion for a purely 2D TS wave and need not concern us here,  $-A^{(f)}$  is the displacement correction at this level and  $\hat{P}^{(f)-}$  gives the corresponding lower-wall pressure contribution. Hence the small pressure difference induced across the channel at this order is given by

$$\hat{p}^{(f)+} - \hat{p}^{(f)-} = -\alpha^2\{\hat{A}^{(f)}I + 2AJ\} + AK \quad (2.13)$$

were  $J \equiv \int_0^1 \bar{u}u^{(3)} dy$  and  $K \equiv \int_0^1 \gamma^{(f)} dy$ . The result (2.13), as expected, is a slight distortion of the earlier pressure jump (2.7), due most significantly to the distortion from the vortex motion.

Lastly here, the longitudinal-vortex flow  $u^{(3)}$ , etc., is controlled on the slower time scale by the equations

$$v_{y^{(3)}} + w_{Z^{(3)}} = 0, \quad (2.14a)$$

$$u_{\bar{T}^{(3)}} + \langle u^{(1)}u_{X^{(1)}} + v^{(1)}u_{y^{(1)}} \rangle + v^{(3)}\bar{u}' = u_{yy^{(3)}}, \quad (2.14b)$$

$$\langle u^{(1)}v_{X^{(1)}} + v^{(1)}v_y^{(1)} \rangle + G_0\bar{u}u^{(3)} = -p_{y^{(3)}}, \quad (2.14c)$$

$$w_{\bar{T}^{(3)}} + \langle u^{(1)}w_{X^{(1)}} + v^{(1)}w_{y^{(1)}} \rangle = -p_{Z^{(3)}} + w_{yy^{(3)}}. \quad (2.14d)$$

Here  $\langle \rangle$  refers to the  $E^0$  component of the enclosed nonlinear terms. Other components  $\propto E, E^2$  (+ c.c.) are also produced but these do not influence the dynamics substantially. Again,  $G_0$  is a scaled Gortler number whose effects could be included in the subsequent analysis although henceforth we take the case of zero  $G_0$  to focus on flat-surface transition. So elimination of  $p^{(3)}$  and manipulation of (2.14) lead to the governing equations

$$(\partial_y^2 - \partial_{\bar{T}})\partial_y^2 v^{(3)} = 4\alpha^2\bar{u}\bar{u}'\partial_Z\{|A|\partial_Z|A|\} \quad (2.15a)$$

$$(\partial_y^2 - \partial_{\bar{T}})u^{(3)} = \bar{u}'v^{(3)} \quad (2.15b)$$

of the longitudinal vortex motion in the core, subject to the boundary conditions

$$u^{(3)} = v^{(3)} = \partial_y v^{(3)} = 0 \text{ at } y = 0, 1 \quad (2.15c)$$

for no slip at the channel walls, in view of (2.14a). There is an implicit assumption here that the induced vortices have little wall-layer structure/modification, and this is borne out by the balances acting in the wall layer as described next.

### 3. THE WALL LAYERS IN TYPE A INTERACTIONS

Viscous wall layers which are in effect critical layers are required near  $y = 0, 1$  to reduce the TS flow, e.g., in (2.4), to rest at the walls. The previous scalings in the core suggest the expansions

$$u = \varepsilon^2 \lambda \tilde{y} + \varepsilon^4 \mu \tilde{y}^2 + \varepsilon^5 U^{(1)} + \varepsilon^6 U^{(3)} + \varepsilon^7 U^{(e)} + \dots + \varepsilon^9 U^{(f)} + \dots, \quad (3.1a)$$

$$v = \varepsilon^8 V^{(1)} + \varepsilon^{10} V^{(e)} + \dots + \varepsilon^{12} V^{(f)} + \dots + \varepsilon^{15} V^{(3)} + \dots \quad (3.1b)$$

$$w = \varepsilon^7 W^{(1)} + \varepsilon^9 W^{(e)} + \varepsilon^{10} W^{(3)} + \dots + \varepsilon^{11} W^{(f)} + \dots \quad (3.1c)$$

$$p = -k_0 \varepsilon^6 X + \varepsilon^7 P^{(1)} + \varepsilon^9 P^{(e)} + \dots + \varepsilon^{11} P^{(f)} + \varepsilon^{12} P^{(3)} + \dots \quad (3.1d)$$

in the lower wall layer near  $y = 0$ , where  $y = \varepsilon^2 \tilde{y}$  with  $\tilde{y}$  of  $O(1)$ , and similarly in the viscous upper wall layer of width  $O(\varepsilon^2)$  adjoining  $y = 1$ . Here  $\lambda = 1$ ,  $\mu = -1$  from the basic flow, while  $U^{(1)}, U^{(e)}, U^{(f)}$  are the induced TS contributions and  $U^{(3)} \equiv \lambda_{3-} \tilde{y}$  is the induced-vortex streamwise shear flow from the core motion, so that  $\lambda_{3-} = \lambda_{3-}(\bar{T}, Z) \equiv \partial_y u^{(3)}$  at  $y = 0+$ . The vortex velocity components  $V^{(3)}, W^{(3)}$  are less simple, being forced by TS-amplitude-squared effects in the wall layer, as in Hall and Smith (1987), although they match with the behavior  $\propto \tilde{y}^2, \tilde{y}$  (plus logarithmic behavior) respectively at large  $\tilde{y}$  required by the core-flow results. Further, the  $\tilde{y}$ -variation in all the pressure terms shown is found to be negligible here, leaving  $P^{(1)} = \hat{P}^{(1)-} E + \text{c.c.}$ , etc., independent of  $\tilde{y}$ . As before, the terms between the  $(e), (f)$  contributions in (3.1a) and so on, including second harmonics  $\propto E^2$ , have no significant impact on the vortex/TS interaction.

The governing equations for  $U^{(1)}$ , for  $W^{(1)}$  and for  $U^{(f)}$  are basically the only ones required now. The first are unsteady, viscous, quasi-2D ones of a TS wave,

$$U_{X^{(1)}} + V_{\tilde{y}^{(1)}} = 0, \quad U_{T^{(1)}} + \lambda \tilde{y} U_{X^{(1)}} + V^{(1)} \lambda = -P_{X^{(1)}} + U_{\tilde{y}^{(1)}} \quad (3.2a, b)$$

subject to

$$U^{(1)} = V^{(1)} = 0 \text{ at } \tilde{y} = 0, \quad U^{(1)} \rightarrow \lambda A \text{ as } \tilde{y} \rightarrow \infty, \quad (3.2c)$$

for no slip and for matching with the core solution. Hence  $U^{(1)} = \hat{U}^{(1)} E + \text{c.c.}$ , etc., where from (3.2a-c) we have, with  $Ai$  denoting the Airy function,

$$\hat{U}_{\xi^{(1)}} = B Ai(\xi), \quad B Ai'_0 = i \alpha \hat{P}^{(1)} \Delta^{-\frac{2}{3}}, \quad (3.3a)$$

$$\lambda A = i \alpha \hat{P}^{(1)} \Delta^{-\frac{2}{3}} \kappa / Ai'_0,$$

where  $\xi = \Delta^{\frac{1}{3}}(\tilde{y} - \Omega/\lambda\alpha)$ ,  $\Delta = \lambda i\alpha$ , the subscript zero denotes evaluation at  $\xi = \xi_0 = -\Delta^{\frac{1}{3}}\Omega/\lambda\alpha$  and  $\kappa = \int_{\xi_0}^{\infty} Ai(q)dq$ . The corresponding upper wall yields the relation

$$-\lambda A = i\alpha \hat{P}^{(1)+} \Delta^{-\frac{2}{3}} \kappa / Ai'_0, \quad (3.3b)$$

on the other hand, due to the opposing displacement effect there, and so coupling (3.3a,b) with the core property (2.7) we obtain the dominant eigenrelation

$$\Delta^{\frac{1}{3}} \kappa \alpha^2 I = 2\lambda^2 Ai'_0 \quad (3.3c)$$

fixing  $\alpha, \Omega$  as both real. Computation gives the values  $\alpha \approx (1.00)(2/I)^{\frac{3}{7}}$ ,  $\Omega \approx (2.298)\alpha^{\frac{2}{3}}$ .

Next, the relatively small spanwise velocity induced,  $W^{(1)}$ , satisfies

$$W_T^{(1)} + \lambda \tilde{y} W_X^{(1)} = -P_Z^{(1)} + W_{\tilde{y}\tilde{y}}^{(1)} \quad (3.4)$$

with  $W^{(1)} = 0$  at  $\tilde{y} = 0$  and  $W^{(1)} \rightarrow 0$  as  $\tilde{y} \rightarrow \infty$ . So  $W^{(1)} = \hat{W}^{(1)}E + \text{c.c.}$  where  $\hat{W}^{(1)}$  is given by

$$\hat{W}^{(1)} = \Delta^{-\frac{2}{3}} \hat{P}_Z^{(1)-} L(\xi) \quad (3.5)$$

and the function  $L(\xi)$  is defined by  $L'' - \xi L = 1$ ,  $L_0 = L(\infty) = 0$ , and is expressible in terms of integrals involving the Airy function.

The extra TS contribution  $U^{(f)}$  is then forced mainly by the slow variation of the primary TS wave, both spanwise in  $Z$  and temporally in  $\bar{T}$ , and by the additional shear from the induced vortex motion. Other contributions are present from the correction  $U^{(e)}$ ,  $V^{(e)}$  in the TS wave but they are less significant. Thus the controlling equations are

$$U_{X^{(f)}} + V_{\tilde{y}}^{(f)} + W_{Z^{(1)}} = 0, \quad (3.6a)$$

$$U_{T^{(f)}} + U_{\bar{T}}^{(1)} + \lambda \tilde{y} U_{X^{(f)}} + \mu \tilde{y}^2 U_{X^{(e)}} + U^{(3)} U_{X^{(1)}} + V^{(1)} U_{X^{(1)}} + V^{(1)} U_{\tilde{y}}^{(3)} \\ + 2V^{(e)} \mu \tilde{y} + V^{(f)} \lambda = -P_X^{(f)} + U_{\tilde{y}\tilde{y}}^{(f)}, \quad (3.6b)$$

subject to the constraints

$$U^{(f)} = V^{(f)} = 0 \text{ at } \tilde{y} = 0, \quad U^{(f)} \rightarrow \lambda A^{(f)} + \lambda_3 - A + \Gamma^{(f)'}(0)A \text{ as } \tilde{y} \rightarrow \infty. \quad (3.6c)$$

The influences of the slow variation and the vortex shear, here and in the upper wall layer, must therefore satisfy a compatibility relation. This can be worked out by solving the system (3.6a-c) for its  $E$ -components, then conducting a similar analysis on the forced contribution in the upper viscous layer, and relating the two via the cross-channel jump condition (2.13)

on the induced wall pressures. After some manipulation, and using the earlier solutions, we obtain the amplitude equation

$$2(Ai_0/\kappa)(\xi_0 + Ai_0'/\kappa)\Delta^{\frac{1}{3}}A_{\bar{T}} = -2\alpha^4\Delta^{-\frac{2}{3}}JA + 2\lambda^2(Ai_0'/\Delta\kappa)A_{ZZ} + \pi_1A - (Ai_0'/\kappa)(\lambda_{3+} + \lambda_{3-})i\alpha[1 - \frac{2}{3}\{\xi_{0^2}(Ai_0/Ai_0') - 1 + \xi_0Ai_0/\kappa\}]A \quad (3.7)$$

governing the effect of the induced vortex motion (through the terms  $J, \lambda_{3\pm}$ ) on the TS amplitude  $A(\bar{T}, Z)$ . In (3.7) the constant  $\pi_1$  is the standard linear-stability contribution for a 2D TS wave, determining whether the flow is sub- or super-critical, while the unknown integral property  $J(\bar{T}, Z)$  and induced shears  $\lambda_{3\pm}(\bar{T}, Z)$  are given by

$$J \equiv \int_0^1 \bar{u}u^{(3)}dy, \quad \lambda_{3-} \equiv \partial_y u^{(3)}(\bar{T}, Z, 0), \quad \lambda_{3+} \equiv -\partial_y u^{(3)}(\bar{T}, Z, 1). \quad (3.8)$$

The equation (3.7) can also be checked against an appropriate expansion of the eigenrelation (3.3c), in fact.

In summary, then, the nonlinear interaction between the warped 2D TS disturbance and the longitudinal vortex motion is controlled by the partial/ordinary differential-cum-integral system consisting of (2.15a-c), (3.7) along with the definitions of  $J, \lambda_{3\pm}$  in (3.8).

#### 4. NONLINEAR TYPE A SOLUTION PROPERTIES; SPECIAL CASES; SECONDARY 3D INSTABILITY; FORMATION OF FOCUSSING

The system governing the nonlinear interaction may be written in the form:

$$(\partial_y^2 - \partial_{\bar{T}})\partial_y^2 v^{(3)} = 2\bar{u} \bar{u}' \partial_Z^2 \rho, \quad (4.1a)$$

$$(\partial_y^2 - \partial_{\bar{T}})u^{(3)} = \bar{u}' v^{(3)}, \quad (4.1b)$$

subject to

$$u^{(3)} = v^{(3)} = \partial_y v^{(3)} = 0 \text{ at } y = 0, 1 \quad (4.1c)$$

and

$$\partial_{\bar{T}} \hat{A} = [c_1 + c_2 J + c_3(\lambda_3^+ + \lambda_3^-)]\hat{A} + c_4 \partial_Z^2 \hat{A}, \quad (4.1d)$$

$$J(\bar{T}, Z) = \int_0^1 \bar{u}u^{(3)}dy; \quad \lambda_3^\pm(\bar{T}, Z) = \mp \partial_y u^{(3)} \text{ at } y = 1, 0; \quad \rho = |\hat{A}|^2. \quad (4.1e)$$

Here  $\hat{A}(\bar{T}, Z) = \alpha A$ , while the constants  $c_2, c_3, c_4$  follow from a computation for the coefficients in (3.7) as

$$c_2 = 131.5 - 175.2i, \quad c_3 = -1.826 - 0.0348i, \quad c_4 = -0.0655 + 0.0873i \quad (4.2)$$

and the constant  $c_1 (\propto \pi_1)$  has positive or negative real part depending on whether the basic flow  $\bar{u} = y(1 - y)$  is super- or sub-critical. As might be expected, there are many features in common between the nonlinear system (4.1) and Hall and Smith's (1987), we note, an exception being the term  $\propto c_4$  in (4.1d) which turns out to have a substantial impact. Again, there is also a connection with Bennett, et al.'s (1988), Hall and Smith's (1989), and Smith's (1988b) work on high-amplitude vortex effects when extreme  $Z$ -variations are considered. The main solution properties of interest are discussed in (a) - (g) below.

(a) First, for an incident TS wave that is only relatively slightly warped we have  $|\partial_Z|$  being small, say  $\partial_Z = \sigma \partial_{\tilde{Z}}$  with  $\sigma$  small and  $\tilde{Z}$  typically  $0(1)$ . Initially then, for example, the vortex flow induced is small,  $0(\sigma^2)$ , and so  $\hat{A}$  grows as an undistorted TS wave like  $\exp(c_1 \bar{T})$  times an arbitrary function of  $\tilde{Z}$ , if  $c_1 > 0$ , and the interaction is weakened. The  $0(\sigma^2)$  vortex motion then amplifies like  $\exp(2c_1 \bar{T})$ , however, being forced by the  $\rho_{ZZ}$  term in (4.1a), and this drives a corresponding  $\exp(3c_1 \bar{T})$  growth in the  $0(\sigma^2)$  correction of the TS wave, via the interaction through  $J, \lambda_3^\pm$  in (4.1d). Hence a fuller interaction comes back into play at increased times  $\bar{T}$  of order  $-\ell n \sigma$ , at which stage  $|\hat{A}|$  is larger, of order  $\sigma^{-1}$ , but the vortex amplitude is also increased, to  $0(1)$ . Since the time variation remains typically  $0(1)$  the full interactive system (4.1a-e) is retrieved at that stage except that the  $c_4 \hat{A}_{ZZ}$  term in (4.1d) is absent due to the slower  $Z$ -variation here. This less-warped case therefore forms a connection with Hall and Smith's (1987), and indeed it is found (see also the later computations and Figure 6) that the interactive system with  $c_4$  in (4.2) replaced by zero yields nonlinear exponential growth of the TS and vortex amplitudes as  $\bar{T}$  increases, in line with the findings of the last-named paper. Specifically, we have here

$$[v^{(3)}, u^{(3)}, \rho, \arg \hat{A}] \sim e^{s\bar{T}} [\bar{v}, \bar{u}, \bar{\rho}, \bar{\phi}] + \dots, \text{ as } \bar{T} \rightarrow \infty, \quad (4.3a)$$

and the nonlinear growth factor  $s$  is determined by the reduced problem obtained from substitution into (4.1) with  $c_4$  zero, namely

$$(\partial_y^2 - s) \partial_y^2 \bar{v} = 2\bar{u} \bar{u}' \partial_y^2 \bar{\rho}, \quad (4.3b)$$

$$(\partial_y^2 - s) \bar{u} = \bar{u}' \bar{v}, \quad (4.3c)$$

$$\bar{u}' = \bar{v} = \partial_y \bar{v} = 0 \text{ at } y = 0, 1, \quad (4.3d)$$

$$c_{2r} \int_0^1 \bar{u} \bar{u}' dy + c_{3r} \{ \partial_y \bar{u}(0, Z) - \partial_y \bar{u}(1, Z) \} = 0. \quad (4.3e)$$

Here (4.3e) follows from the dominant terms of order  $\exp(3s\bar{T}/2)$  that appear in (4.1d) when (4.3a) holds. The profile  $\bar{\rho}(Z)$  remains arbitrary, although we observe that (4.3a-e)

represents an exact solution of (4.1) when  $c_1 = c_4 = 0$ , in which event  $\bar{\rho}(Z)$  is fixed by the initial distribution. The eigenvalue  $s$  is one of those determined by Hall and Smith (1987).

(b) Next, suppose that  $c_1$  is small, corresponding to a state which is closer to neutral than the above, e.g., if  $c_1$  is positive this occurs at a lower Reynolds number, for a prescribed wavenumber. Then the less-warped case initially has

$$\hat{A} = a_0(\tilde{T}, \tilde{Z}) + \sigma^2 \hat{A}_1(\bar{T}, \tilde{T}, \tilde{Z}) + \dots \quad (4.4a)$$

where  $\partial_{\bar{T}} \rightarrow \partial_{\bar{T}} + \sigma^2 \partial_{\tilde{T}}$  and

$$\hat{A}_{1\bar{T}} + a_{0\tilde{T}} = [\tilde{c}_1 + c_2 \tilde{J} + c_3(\tilde{\lambda}_3^+ + \tilde{\lambda}_3^-)] a_0 + c_4 a_{0\tilde{Z}\tilde{Z}} \quad (4.4b)$$

from (4.1d), whereas (4.1a,b) lead to

$$(\partial_y^2 - \partial_{\bar{T}}) \partial_y^2 \tilde{v}^{(3)} = 2\bar{u} \bar{u}' \rho_{0\tilde{Z}\tilde{Z}}, (\partial_y^2 - \partial_{\bar{T}}) \tilde{u}^{(3)} = \bar{u}' \tilde{v}^{(3)}. \quad (4.4c, d)$$

Here

$$[u^{(3)}, v^{(3)}, J, \lambda_3] = \sigma^2 [\tilde{u}^{(3)}, \tilde{v}^{(3)}, \tilde{J}, \tilde{\lambda}_3], \quad (4.4e)$$

$c_1 = \sigma^2 \tilde{c}_1$ , and  $\rho_0 = |a_0|^2$ . Apart from transients, the correction term  $\hat{A}_1$  grows exponentially with time [or  $a_0$  does] and so at a later stage we have effectively the ordering

$$\hat{A} = 0(1), \quad \partial_Z = \sigma \partial_{\tilde{Z}}, \quad \partial_{\bar{T}} = \sigma^2 \partial_{\tilde{T}}, \quad (4.5)$$

along with (4.4e). Thus the governing equations now reduce to

$$\partial_y^2 \tilde{v}^{(3)} = 2\bar{u} \bar{u}' \rho_{\tilde{Z}\tilde{Z}}, \quad \partial_y^2 \tilde{u}^{(3)} = \bar{u}' \tilde{v}^{(3)}, \quad (4.6a, b)$$

$$\hat{A}_{\tilde{T}} = [\tilde{c}_1 + c_2 \tilde{J} + c_3(\tilde{\lambda}_3^+ + \tilde{\lambda}_3^-)] \hat{A} + c_4 \hat{A}_{\tilde{Z}\tilde{Z}}, \quad (4.6c)$$

since the time scale is relatively slow here. The boundary conditions on (4.6a,b) are that  $\tilde{u}^{(3)}, \tilde{v}^{(3)}, \partial_y \tilde{v}^{(3)}$  vanish at  $y = 0, 1$  and the solution is straightforward, giving

$$\tilde{v}^{(3)} = \{2y^7 - 7y^6 + 7y^5 - 3y^3 + y^2\}/420, \quad (4.7a)$$

$$\begin{aligned} \tilde{u}^{(3)} = & \{-y^{10}/45 + y^9/9 - 3y^8/16 + y^7/12 + y^6/10 \\ & -y^5/8 + y^4/24 - 1/720\}/210 \end{aligned} \quad (4.7b)$$

explicitly; hence the vortex properties  $\tilde{J}, \tilde{\lambda}_3$  can be evaluated and substituted into (4.6c). The resulting complex amplitude equation for  $\hat{A}(\tilde{T}, \tilde{Z})$  is then

$$\hat{A}_{\tilde{T}} = [\tilde{c}_1 + b_1 \rho_{\tilde{Z}\tilde{Z}}] \hat{A} + c_4 \hat{A}_{\tilde{Z}\tilde{Z}}, \quad (4.8a)$$

$$\rho = |\hat{A}|^2 \quad (4.8b)$$

where

$$b_1 = (-0.486 + 3.905i)10^{-5}. \quad (4.9)$$

We address this simplified nonlinear version, (4.8a,b), now because to some extent it mirrors the main properties of the full system (4.1). It is vaguely like certain well-studied equations such as the cubic Schrodinger equation, incidentally, although in general no firmer connection seems available.

One particular solution is simply that for 2D flow of course where  $\hat{A} = A_0(\tilde{T})$  is independent of  $\tilde{Z}$ , and there (4.8a) yields the exponential form  $\tilde{A}_0 = \exp(\tilde{c}_1\tilde{T})$  in line with the definition of  $\tilde{c}_1$ . To examine the stability of this 2D solution to small 3D distortions we use the polar form  $\hat{A} = r \exp(i\theta)$  with  $(r, \theta)$  ( $\tilde{T}, \tilde{Z}$ ) real, convert (4.8) to two real coupled nonlinear equations for  $r, \theta$ ,

$$r_{\tilde{T}} = (\tilde{c}_{1r} + b_{1r}\rho_{\tilde{Z}\tilde{Z}})r + c_{4r}(r_{\tilde{Z}\tilde{Z}} - r\theta_{\tilde{Z}}^2) - c_{4i}(r^2\theta_{\tilde{Z}})_{\tilde{Z}}/r[\rho \equiv r^2], \quad (4.10a)$$

$$r\theta_{\tilde{T}} = (\tilde{c}_{1i} + b_{1i}\rho_{\tilde{Z}\tilde{Z}})r + c_{4i}(r_{\tilde{Z}\tilde{Z}} - r\theta_{\tilde{Z}}^2) + c_{4r}(r^2\theta_{\tilde{Z}})_{\tilde{Z}}/r \quad (4.10b)$$

and then expand, with  $\delta$  small,

$$(r, \theta) = \{\gamma_0 e^{\tilde{c}_{1r}\tilde{T}}, \theta_0 + \tilde{c}_{1i}\tilde{T}\} + \delta(r_1, \phi_1) + 0(\delta^2). \quad (4.11a)$$

The expression in curly brackets is the 2D solution, with  $\gamma_0(> 0), \theta_0$  prescribed constants, and of course  $\rho = \rho_0 + \delta\rho_1 + 0(\delta^2)$  where  $\rho_0 = \gamma_0^2 \exp(2\tilde{c}_{1r}\tilde{T}), \rho_1 = 2\gamma_0 r_1 \exp(\tilde{c}_{1r}\tilde{T})$ . The linearized system resulting from substitution of (4.11a) into (4.10) yields solutions

$$(r_1, \phi_1) \propto \exp(i\tilde{\beta}\tilde{Z}) \exp(\tilde{Q}\tilde{T}) \quad (4.11b)$$

for small  $\tilde{c}_{1r}$  or, at large times, for  $\tilde{c}_{1r}$  negative, and a similar result holds for  $\tilde{c}_{1r}$  positive. Here  $\tilde{\beta}$  is the particular spanwise wavenumber of the 3D distortion and the effective growth-rate  $\tilde{Q}$  is found to be given by

$$\tilde{Q} = \tilde{c}_{1r} - \tilde{\beta}^2(b_{1r}\rho_0 + c_{4r}) \pm \tilde{\beta}\{b_{1r}^2\rho_0^2\tilde{\beta}^2 - 4b_{1r}\rho_0\tilde{c}_{1r} - 2\tilde{\beta}^2 b_{1i}\rho_0 c_{4i} - \tilde{\beta}^2 c_{4i}^2\}^{\frac{1}{2}}. \quad (4.11c)$$

The dependence of  $\tilde{Q}_r$  on  $\tilde{\beta}$  and the 2D wave amplitude  $\rho_0$  is presented in Figure 2. Several points emerge here but the main ones are the following. First, the secondary 3D instability is very pronounced, especially for increased  $\tilde{\beta}$  and/or  $\rho_0$  where  $\max \tilde{Q}_r$  increases like  $\tilde{\beta}^2\rho_0$  approximately. Thus both the effects of three-dimensionality and of 2D amplitude growth act in concert to destabilize, accentuating the secondary distortion or warping. The next point is that the secondary 3D instability here is quite different as a rule from Herbert's

(1984) suggested form and is associated more with the 3D growth-rate behavior at large Reynolds numbers, through the  $c_{4r}$  term above, than with the induced-vortex/Squire-mode response through  $b_1\rho_0$ , c.f. Section 6 below. The latter effect dominates only if  $c_4$  is negligible as in item (a) earlier corresponding to reduced three-dimensionality in the initial input, this giving a loose connection with Squire-mode destabilization. Although there is therefore some dependence on the initial conditions of course, in general the enhancement of any warping is due mainly to the  $c_{4r}$  contribution. Third, this can occur even while the flow is subcritical. Fourth, the increase in temporal growth rate with increasing  $\tilde{\beta}$  is so fast that for an initial-value problem in general, where (4.11b) is replaced by a spectral decomposition in  $\tilde{Z}$  for instance and in effect integration with respect to  $\tilde{\beta}$  becomes appropriate, the 3D distortion becomes singular within a finite time. This is similar to the break-up phenomenon associated with the backward heat-conduction equation. In the present case the break-up takes place with a time scale  $\propto \tilde{Q}^{-1}$  or  $\tilde{\beta}^{-2}$ , typically, i.e., focusing occurs with  $|\tilde{Z} - \tilde{Z}_S| \propto (\tilde{T}_S - \tilde{T})^{\frac{1}{2}}$  at a finite time  $\tilde{T}_S$  and location  $\tilde{Z}_S$ . The local behavior there is given by a similarity form which is analogous to that in (4.13) below and is somewhat dependent on the initial conditions. If these or the boundary conditions are unrestricted then the linearized initial-value problem can become ill-posed in the sense that effectively  $\tilde{T}_S$  tends to zero. This cumulative instability for large wavenumbers  $\tilde{\beta}$  and/or large amplitudes  $\rho_0$  is due in the present regime to  $b_{1r}, c_{4r}$  being negative but it permeates the analysis and computations in the other regimes studied as well.

Another simple particular solution should also be mentioned, namely the single mode  $\hat{A} = \tilde{A}_0(\tilde{T}) \exp(i\beta\tilde{Z})$  with  $\beta$  fixed, giving an extension of the previous one and yielding to similar analysis. Here in addition  $\rho = |\tilde{A}_0|^2 = \rho(\tilde{T})$  and so  $\tilde{A}_0(\tilde{T})$  satisfies the linear equation

$$\tilde{A}'_0 = (\tilde{c}_1 - c_4\beta^2)\tilde{A}_0. \quad (4.12)$$

This further illustrates the strong instability possible since, as  $c_{4r}$  is negative, the solution  $\propto \exp((\tilde{c}_1 - c_4\beta^2)\tilde{T})$  grows exponentially for  $(-c_{4r})\beta^2 + \tilde{c}_{1r}$  positive and the growth rate increases indefinitely with increasing spanwise wavenumber  $\beta$ . Limit-cycle solutions may also be sought but they are probably, although not necessarily, irrelevant in view of the more general behavior proposed next.

The aspects above suggest that the most common response of the system (4.8a,b) is likely to be a nonlinear break-up within a finite time,  $\tilde{T}_1$  say. The orders of magnitude involved indicate that as  $\tilde{T} \rightarrow \tilde{T}_1^-$  the singular behavior has

$$\hat{A} \sim \left| \frac{c_4}{b_1} \right|^{\frac{1}{2}} \tilde{a}(\eta), \quad \rho \sim \left| \frac{c_4}{b_1} \right| \tilde{\rho}(\eta) \quad \text{and} \quad \eta = |c_4|^{\frac{1}{2}} (\tilde{Z} - \tilde{Z}_1) / (\tilde{T}_1 - \tilde{T})^{\frac{1}{2}} \quad (4.13a - c)$$



focussed around the position  $\tilde{Z} = \tilde{Z}_1$ . There, from (4.8a,b), the functions  $\tilde{a}(\eta), \tilde{\rho}(\eta)$  satisfy

$$\frac{1}{2}\eta\tilde{a}' = \tilde{\rho}''\tilde{a}\exp(i\phi_1) + \tilde{a}''\exp(i\phi_2), \quad \tilde{\rho} = |\tilde{a}|^2, \quad (4.14a, b)$$

subject to  $\tilde{a}, \tilde{\rho}$  being bounded at large  $|\eta|$ , to match with the flow away from  $\tilde{Z} \approx \tilde{Z}_1$ , and with  $\phi_1 = \arg(b_1), \phi_2 = \arg(c_4)$  so that  $\pi/2 < \phi_{1,2} < \pi$ . The localized behavior here produces a shock-like jump from  $\tilde{a}(-\infty) = \tilde{a}_0$  to  $\tilde{a}(\infty) = \tilde{a}_1$ , i.e., at  $\tilde{Z} = \tilde{Z}_1 \pm$ . For example, if the jump is small then (4.14a,b) yield the result

$$\tilde{\rho} - \tilde{\rho}_0 = \int_{-\infty}^{\eta} \exp(-N\eta^2) d\eta \quad (4.15a)$$

where

$$N = [-(\tilde{\rho}_0\hat{c}_1 + \hat{c}_2)\hat{c}_1 \pm \{(\tilde{\rho}_0\hat{c}_1^2 - \hat{s}_1\hat{s}_2)^2 - \hat{s}_2^2\}^{\frac{1}{2}}] \\ / [4\hat{c}_1\{1 + 2\tilde{\rho}_0\cos(\phi_1 - \phi_2)\}] \quad (4.15b)$$

and  $\hat{c}_n \equiv \cos\phi_n < 0$ ,  $\hat{s}_n \equiv \sin\phi_n > 0$ ,  $n = 1, 2$ . As each root  $N$  has positive real part the solution (4.15a) is acceptable and the proposed jump behavior is obtained from  $\eta = -\infty$  to  $\eta = +\infty$ . As regards other acceptable forms, numerical solutions of (4.14a,b) for a range of jump conditions were derived by use of a finite-difference procedure and these are shown in Figure 3. They agree well with (4.15) for small jumps. The description (4.13) - (4.14) of a local nonlinear break-up also gains weight from the fact that, at least for zero  $\tilde{c}_1$ , it provides an exact similarity solution of the system (4.8a,b). The occurrence of the break-up here provides the means for the less-warped interaction to focus and acquire the full form (4.1a-e), leading on to the subsequent response studied in (f), (g) below.

(c) The single-mode solution mentioned in (b) above may be extended to the full nonlinear system (4.1a-e), since if  $\hat{A} = \tilde{A}_0(\bar{T})\exp(i\beta Z)$  then  $\tilde{A}_0$  is governed by (4.12) again provided  $\tilde{c}_1$  is replaced by  $c_1$ . So the comments immediately following (4.12) apply also to the general case.

(d) Likewise, secondary 3D instability can be established for the full system by extension of the approach in (4.10) - (4.11). For the full system (4.1) we use polars in the form  $\hat{A} = R\exp(i\phi)$  to replace (4.1d) by the two real equations

$$R_{\bar{T}} = [c_{1r} + c_{2r}J + c_{3r}(\lambda_3^+ + \lambda_3^-)]R + c_{4r}[R_{ZZ} - R\phi_Z^2] \\ - c_{4i}(R^2\phi_Z)_Z/R, \quad (4.16a)$$

$$R\phi_{\bar{T}} = [c_{1i} + c_{2i}J + c_{3i}(\lambda_3^+ + \lambda_3^-)]R + c_{4i}[R_{ZZ} - R\phi_Z^2] \\ + c_{4r}(R^2\phi_Z)_Z/R \quad (4.16b)$$

with  $\rho = R^2$  now, and then the secondary 3D instability of the 2D TS solution  $R = \Gamma_0 \exp(c_{1r}\bar{T})$ ,  $\phi = \phi_0 + c_{1i}\bar{T}$  [where  $\Gamma_0, \phi_0$  are constants,  $\Gamma_0 > 0$ ] is examined by perturbing it, for small  $\delta$ ,

$$(R, \phi) = \{\Gamma_0 \exp(c_{1r}\bar{T}), \phi_0 + c_{1i}\bar{T}\} + \delta(R_1, \phi_1) + 0(\delta^2), \quad (4.17a)$$

$$(u^{(3)}, v^{(3)}) = \delta(u_1^{(3)}, v_1^{(3)}) + 0(\delta^2).$$

The resulting linearized system for  $R_1, \phi_1$  is found to yield both fast growth in the form

$$R_1 \approx \exp[\gamma \exp(2c_{1r}\bar{T}/3)] \quad (\gamma = \text{constant}) \quad (4.17b)$$

at large times, as might be expected, and fast growth for increasing spanwise wavenumbers  $\beta$ . The latter growth is analogous to that in item (b) above, causing a finite-time breakdown of the small 3D distortion in (4.17a) for an initial-value problem and making the subsequent computational work very sensitive.

(e) An extreme case of interest opposite to those in (a), (b) arises for relatively large amplitudes and short spanwise lengths  $|Z|$ , such that  $Z$  is  $0(\Gamma)$  say with  $\Gamma \ll 1$ . Then if  $|\hat{A}|$  is  $0(\Gamma^{-2})$ ,  $\rho$  is  $0(\Gamma^{-4})$  and the balances in (4.1a-e) suggest that typically the time scale  $\bar{T}$  is fast,  $0(\Gamma^2)$ , with  $v^{(3)} \sim \Gamma^{-4}$  and  $u^{(3)} \sim \Gamma^{-2} \sim \lambda_3^\pm \sim J$  all being large in magnitude. This has the effect of rendering the core flow of (4.1a,b) inviscid, apart from two wall layers of width  $0(\Gamma)$  in  $y$ , which influence the values of  $\lambda_3^\pm$ , and of replacing  $c_1$  in (4.1d) by zero. The resulting simplified system then ties in closely with the analysis in (g) below.

(f) Computational studies of the full nonlinear system (4.1a-e) (with (4.2)) have been made, applying both spectral and finite-difference approaches, for various starting conditions imposed at time  $\bar{T} = 0$  and for various values of the constant  $c_1$ . IN the spectral treatment Fourier series in  $Z$  of period  $L$  were substituted into (4.1a-e) to yield a set of coupled nonlinear equations in  $y, \bar{T}$  for the Fourier components. The set was truncated at a large number ( $M$ ) of terms and marched forward in time steps  $\Delta\bar{T}$  with a predictor-corrector method of second-order accuracy in  $y, \bar{T}$ , for grid sizes  $\Delta y$  in  $y$ . A range of values for the parameters  $L, M, \Delta\bar{T}, \Delta y$  was also examined, and Figure 4 shows a typical result. Similarly, Figure 5 presents a typical computation from the finite-difference procedure, where time-stepping was applied as before but central differences were taken in both  $y$  and  $Z$  (step size  $\Delta Z$ ). The results from both methods tend to confirm the analytical features that we have described previously, with the properties of shortest spanwise scale growing the fastest temporally. This leads on to the account in (g) below.

The reduced system implied in (a) above, i.e., (4.1a-e), (4.2) but with  $c_4$  replaced by zero, has also been studied computationally and a representative result is given in Figure 6,

obtained from the spectral approach. The secondary 3D instability analogous to (4.11a-c) is much reduced now and the cascade of energy into higher spanwise components mentioned in the last paragraph is not observed; instead the nonlinear amplitude growth computed appears to be consistent with the description in (a) above, that is, the TS wave and the vortex flow amplify together exponentially.

(g) The terminal behavior of the full system (4.1a-e), (4.2) is considered now. Many types of algebraic or exponential nonlinear breakdown suggest themselves and have been tried by us,<sup>4</sup> and the same goes for additional special cases, but the favorite description, guided by the features (a) - (f) above, is as follows.

We propose that the nonlinear interaction breaks up by producing a concentrated “tongue” formation within a finite time  $\bar{T} = \bar{T}_s$ : see Figure 7. The orders of magnitude suggest then the singular behavior

$$R \equiv |\hat{A}| \sim (\bar{T}_s - \bar{T})^{-1} \tilde{R}(\tilde{z}), \quad \rho \sim (\bar{T}_s - \bar{T})^{-2} \tilde{\rho}(\tilde{z}), \quad (4.18a, b)$$

$$u^{(3)} \sim (\bar{T}_s - \bar{T})^{-1} \tilde{u}(y, \tilde{z}), \quad v^{(3)} \sim (\bar{T}_s - \bar{T})^{-2} \tilde{v}(\tilde{y}, \tilde{z}), \quad (4.18c, d)$$

$$\phi \sim G \ln(\bar{T}_s - \bar{T}) + \tilde{\phi}(\tilde{z}) \quad (4.18e)$$

to leading order as  $\bar{T} \rightarrow \bar{T}_s^-$ , with the dependence on  $y, \tilde{z}$  as shown, and with the tongue being focussed within a distance  $0(\bar{T}_s - \bar{T})^{\frac{1}{2}}$  of the spanwise location  $Z = Z_s$  say, so that

$$Z - Z_s = (\bar{T}_s - \bar{T})^{\frac{1}{2}} \tilde{z} \quad (4.18f)$$

where  $\tilde{z}$  is  $0(1)$ . The algebraic break-up (4.18a-f) can be generalized readily, but the particular scales shown above appear to be the favored ones: c.f. (4.13). Also here, the vortex response (4.18c,d) applies in the bulk (i) ( $0 < y < 1$ ) of the flow, where the vortex becomes mainly inviscid, whereas new viscous wall layers (ii) of width  $\propto (\bar{T}_s - \bar{T})^{\frac{1}{2}}$  come into play near  $y = 0, 1$  in which  $u^{(3)}, v^{(3)}$  reduce in magnitude to the levels  $(\bar{T}_s - \bar{T})^{-\frac{1}{2}}, (\bar{T}_s - \bar{T})^{-\frac{3}{2}}$  in turn. The vortex skin-friction contributions  $\lambda_3^\pm$  are determined by the properties in those wall layers (ii) but the vortex’s coanda effect  $J$  is dominated by the contribution from the bulk (i), and so viscous-inviscid interaction maintains itself during the tongue development. The governing equations (4.1a,b) for the vortex motion become

$$(-2 - \tilde{z} \partial_{\tilde{z}}/2) \partial_y^2 \tilde{v} = 2\bar{u} \bar{u}' \tilde{\rho}_{\tilde{z}\tilde{z}}, \quad (4.19a)$$

$$(-1 - \tilde{z} \partial_{\tilde{z}}/2) \tilde{u} = \bar{u}' \tilde{v}, \quad (4.19b)$$

---

<sup>4</sup>For example, the nonlinear exponential growth in (4.3) can be seen to apply in principle to the full system also, this growth then providing a match with our related work, Bennett, et al. (1988), Hall and Smith (1989), Smith (1988b) on the long-scale vortex/wave interactions.

subject to  $\tilde{u} = \tilde{v} = 0$  at  $y = 0, 1$ , while the TS part satisfies [with  $\tilde{\rho} = \tilde{R}^2$ ]

$$\tilde{R} + \tilde{z}\tilde{R}_{\tilde{z}}/2 = [c_{2r}\tilde{J} + c_{3r}(\tilde{\lambda}_3^+ + \tilde{\lambda}_3^-)]\tilde{R} + c_{4r}(\tilde{R}_{\tilde{z}\tilde{z}} - \tilde{R}\tilde{\phi}_{\tilde{z}}^2) - c_{4i}(\tilde{R}^2\tilde{\phi}_{\tilde{z}})_{\tilde{z}}/\tilde{R}, \quad (4.19c)$$

$$\tilde{R}(\tilde{z}\tilde{\phi}_{\tilde{z}}/2 - G) = [c_{2i}\tilde{J} + c_{3i}(\tilde{\lambda}_3^+ + \tilde{\lambda}_3^-)]\tilde{R} + c_{4r}(\tilde{R}^2\tilde{\phi}_{\tilde{z}})_{\tilde{z}}/\tilde{R} + c_{4i}(\tilde{R}_{\tilde{z}\tilde{z}} - \tilde{R}\tilde{\phi}_{\tilde{z}}^2) \quad (4.19d)$$

and, again to leading order,  $J \sim (\bar{T}_s - \bar{T})^{-1}\tilde{J}(\tilde{z})$ ,  $\lambda_3^\pm \sim (\bar{T}_s - \bar{T})^{-1}\tilde{\lambda}_3^\pm(\tilde{z})$  with

$$\tilde{J} = \int_0^1 \bar{u}\tilde{u}dy. \quad (4.19e)$$

The skin friction terms  $\tilde{\lambda}_3^\pm$ , however, are affected by the wall layers (ii) which are required to reduce  $\partial_y\tilde{v}$  to zero at  $y = 0, 1$ . A solution of the terminal problem (4.19) may then be sought in the separated-variables manner:

$$[\tilde{v}, \tilde{u}] = [V_a(y)V_b(\tilde{z}), U_a(y)U_b(\tilde{z})]. \quad (4.20a)$$

Thus (4.19a,b) split into the ordinary differential equations

$$V_a'' = 2k\bar{u}\tilde{u}', \quad (-2V_b - \tilde{z}V_b'/2) = k^{-1}\tilde{\rho}'' \quad (4.20b)$$

$$U_a = \ell\bar{u}'V_a, \quad (-U_b - \tilde{z}U_b'/2) = \ell^{-1}V_b \quad (4.20c)$$

where  $U_a, V_a$  are to vanish at  $y = 0, 1$ , the prime denote differentiation with respect to  $y$  or  $\tilde{z}$  as appropriate and  $k, \ell$  are constants. Equations (4.19c,d) remain intact here provided that  $(\tilde{J}, \tilde{\lambda}_3^\pm)$  is replaced by

$$(J_a, \lambda_a^\pm)U_b(\tilde{z}) \text{ with } J_a \equiv \int_0^1 \bar{u}U_a dy. \quad (4.20d)$$

The solution for  $V_a$  is

$$V_a = k\left\{\int_0^y \bar{u}^2 dy - y \int_0^1 \bar{u}^2 dy\right\}, \quad (4.21a)$$

from which  $U_a$  follows in (4.20c), giving  $J_a$  in (4.20d) equal to  $-k\ell/4200$ . In contrast,  $V_b, U_b$  are given implicitly by

$$V_b = -2k^{-1}\tilde{z}^{-4} \int_0^{\tilde{z}} z^3 \tilde{\rho}''(z) dz, \quad U_b = -2\ell^{-1}\tilde{z}^{-4} \int_0^{\tilde{z}} z^3 V_b(z) dz, \quad (4.21b, c)$$

the origin of integration being zero to avoid an irregularity in general. Hence the terminal response may be reduced in principle to the solution of a pair of integro-differential equations for  $\tilde{R}, \tilde{\phi}$  (using  $\tilde{\rho} \equiv \tilde{R}^2$ ) as functions of  $\tilde{z}$  in the range  $-\infty < \tilde{z} < \infty$ , by substitution of (4.20d) - (4.21c) into (4.19c,d). Local expressions valid for small  $|\tilde{z}|$  in the center of the tongue can be written down and allow the solution to be symmetric there. In the other extreme, at the edges of the tongue as  $\tilde{z} \rightarrow \pm\infty$ , the vortex and TS amplitudes tend to zero, specifically in the form

$$\tilde{R} \sim R_0\tilde{z}^{-2} + R_1\tilde{z}^{-4} + \dots, \quad \tilde{\rho} \sim \rho_0\tilde{z}^{-4} + \rho_1\tilde{z}^{-6} + \dots, \quad (4.22a, b)$$

$$\tilde{\phi} \sim 2G\ell n|\tilde{z}| + \Phi_1 \tilde{z}^{-2} + \dots, \quad (4.22c)$$

$$V_b \sim a_0 \tilde{z}^{-4} + a_1 \tilde{z}^{-6} + \dots, \quad U_b \sim b_0 \tilde{z}^{-2} + b_1 \tilde{z}^{-4} + \dots, \quad (4.22d, e)$$

consistent with the controlling equations above. Here  $R_0, R_1, \rho_0, \rho_1, \Phi_1, a_0, a_1, b_0, b_1$  are constants. The complete behavior in (4.22) then matches with the less pronounced flow outside the tongue where the amplitudes  $|\hat{A}|, |v^{(3)}|, |u^{(3)}|$  and the phase  $\phi$  are all  $0(1)$  at  $0(1)$  distances from  $Z = Z_s$ .

Thus the streak pattern of (4.18a-f) appears to provide a self-consistent terminal response to the nonlinear interaction. The pattern is in fact another nominally exact solution of the full system (4.1a-e), (4.2) if the TS linear-growth term  $c_1$  is neglected. A particular type of this terminal form we note has the TS amplitude dominating, equivalent to  $|\tilde{J}|, |\tilde{\lambda}_3^\pm|$  being relatively small in (4.19c,d), in which case we find the solution

$$\tilde{R} \exp(i\tilde{\phi}) = d_1 [2c_4 + \tilde{z} \exp(\tilde{z}^2/4c_4) \int_{d_2}^{\tilde{z}} \exp(-\hat{z}^2/4c_4) d\hat{z}] \quad (4.22)$$

where  $d_1, d_2$  are constants. This yields an acceptable tongue response, in agreement with (4.21), since  $c_{4r}$  is negative. A similar TS-dominated break-up can be proposed by suitable adjustment of the algebraic forms in (4.18) as indicated earlier but that yields a weaker and apparently less likely singularity. Extension of (4.22) to incorporate the vortex effect more fully can be made by expanding about (4.22) or solving the entire terminal system in its integro-differential form described above, analogous to the break-up features in (b).

The implications of items (e), (g) in particular are discussed in the next section.

## 5. REPERCUSSIONS, AND THE TYPE B INTERACTION

The main repercussion follows from the findings in (g) in the previous section and concerns the next stage in the evolution of the typical vorticity tongue in the channel flow. This seems to occur when the spanwise scale  $|z|$  of the streak reduces to  $0(\varepsilon^{-2})$ , for the following reason. The relative effect in the TS wave due to its slow growth and to the influence of the induced vortex is of order  $\varepsilon^4$  [see Section 2] but becomes accentuated like  $|\lambda_3^\pm| [(\alpha (\bar{T}_s - \bar{T})^{-1})]$  typically as the break-up takes control. In contrast, the relative effect from classical amplitude-cubed contributions is smaller, of order  $\varepsilon^6$ , but proportional to  $|A|^2$  say, i.e.  $\propto \varepsilon^6 (\bar{T}_s - \bar{T})^{-2}$ , as the break-up is approached. Therefore the two effects become comparable when the scaled time  $\bar{T} - \bar{T}_s$  decreases to  $0(\varepsilon^2)$ , corresponding to the  $z$ -scale of  $0(\varepsilon^{-2})$  on account of (g) above. The next stage then, labelled Type b, has an increased vortex amplitude, with

$$(u, v, w) = (\bar{u}, 0, 0) + 0(\varepsilon^2, \varepsilon^7, \varepsilon^5) \text{ (vortex)} \quad (5.1)$$

in the core, an increased TS amplitude of the form

$$(u, p) = (\varepsilon^2 \lambda Y, 0) + 0(\varepsilon^3, \varepsilon^5) \text{ (TS)} \quad (5.2)$$

in the two  $0(\varepsilon^2)$ -thick viscous wall layers, and buffer zones of width  $0(\varepsilon)$  in which the skin friction of the vortex flow is determined. The multiple scaling also alters from that in Section 2 to

$$(\partial_t, \partial_x, \partial_z) \rightarrow (\varepsilon^3 \partial_T + \varepsilon^5 \partial_{T_1}, \varepsilon \partial_X, \varepsilon^2 \partial_{Z_1}). \quad (5.3)$$

Hence the effects of the vortex skin friction and momentum integral ( $\propto J$ ) compared with those of the basic flow are  $0(\varepsilon^2)$ , interacting with the new slow-temporal and warping effects in (5.3) and with the  $0(\varepsilon^2)$  amplitude-squared influence that the TS wave exerts in producing the vortex motion. In addition, amplitude-cubed effects of relative size  $0(\varepsilon^2)$  now also enter as a major new physical contribution in the reckoning of the TS amplitude itself. This stage is sketched structurally in Figure 8 and merits further study, in particular to see if the spanwise focusing observed in the nonlinear interaction Type a continues through the next stage, Type b.

A similar inference holds if, in the spirit of item (e) in Section 4, we turn to consider different starting conditions. As the effective amplitude  $\Gamma^{-1}$  is increased the next distinct stage encountered is exactly that of (5.1)-(5.3). Reduced warping in the input flow, on the other hand, as in item (a), can lead to a much slower nonlinear-exponential evolution of the interaction as time increases, more similar to that found in Hall and Smith (1987). This slower evolution applies to the full system as well, as the footnote to item (g) mentions [see also additional comments on initial conditions and by-pass processes in Smith, 1988b], and the exponential form links up with our related work (Bennett, et al., 1989), referred to more fully in the next section.

## 6. NONLINEAR INTERACTION, TYPES C, D, E

The earlier sections have shown two related Types a,b of nonlinear interaction to be possible. We turn now to the alternative vortex/wave interactions c,d,e which can arise from different input conditions as follows.

First, we consider Types c,d, which emerge from the 3D interactive three-layer structure based on the  $\varepsilon^{-1}$  length scale in  $x$  (Smith, 1980). The flow solutions in the three layers have the expansions

$$[u, v, w, p] = \begin{cases} [\varepsilon^2 U, \varepsilon^5 V, \varepsilon^2 W, \varepsilon^4 P]^+, y = 1 - \varepsilon^2 Y^+, \\ [\bar{u} + \varepsilon^2 A \bar{u}', -\varepsilon A_X \bar{u}, 0(\varepsilon^4), 0(\varepsilon^4)], y = 0(1), \\ [\varepsilon^2 U, \varepsilon^5 V, \varepsilon^2 W, \varepsilon^4 P]^-, y = \varepsilon^2 Y^-, \end{cases}$$

to the orders shown, with the unknown pressures  $P^\pm$  independent of  $Y^\pm$  in turn and now  $(x, z) = \epsilon^{-1}(X, Z)$ ,  $t = \epsilon^{-3}T$  where again  $\epsilon \equiv \text{Re}^{-\frac{1}{7}}$ . Hence the governing equations in the two wall layers are the 3D unsteady interactive-boundary-layer equations,

$$[U_X + V_Y + W_Z]^\pm = 0, \quad (6.2a)$$

$$[U_T + UU_X + VU_Y + WU_Z]^\pm = -P_X^\pm(X, Z, T) + U_{YY}^\pm, \quad (6.2b)$$

$$[W_T + UW_X + VW_Y + WW_Z]^\pm = -P_Z^\pm(X, Z, T) + W_{YY}^\pm \quad (6.2c)$$

subject to no slip at  $Y^\pm = 0$  and

$$U^\pm \sim Y^\pm \mp A(X, Z, T), W^\pm \rightarrow 0, \text{ as } Y^\pm \rightarrow \infty, \quad (6.2d)$$

with  $-A$  representing the unknown core-flow displacement. The pressure-displacement law necessary to close the system comes from the core-flow dynamics (c.f. Section 2), giving

$$P^+ - P^- = IA_{XX} \quad (6.2e)$$

where again  $I = 1/30$ . The 3D fully nonlinear formulation (6.2a-e) is the counterpart of the 3D triple-deck formulation in boundary layers (see e.g., Hall and Smith, 1984, 1988) and in general it requires a computational treatment (e.g., Smith, 1989), while a possibility for its ultimate behavior is the finite-time singularity of Smith (1988a).

The emergence of vortex/TS nonlinear interaction from within the system (6.2) is addressed next, along the lines of the simultaneous work by Smith (1988b), although here temporal rather than spatial evolution is of concern. An order-of-magnitude argument establishes the main possibilities. Thus, if the warping factor is  $\beta(\sim \partial_Z)$  then for an input wave amplitude  $0(h)$  the relative effects present, compared with 2D theory, are

$$\beta^2, h^2, h^2\beta^2k^{-1}, k, \quad (6.3a - d)$$

due to warping, to the disturbance size, to the induced vortex-shear influence, and to the slow temporal dependence ( $k$ ) of the vortex, respectively. Here the third contributions stems from the feature that the velocity  $W$  of the induced vortex for  $Y$  of order unity is  $0(h^2\beta)$ , for either wall layer, and it remains at that level (apart from a logarithmic factor) in the vortex-dominated outer zone or buffer which is induced where  $Y \sim k^{-\frac{1}{2}}$  is large, for an unsteady-viscous force balance in the vortex motion. In consequence, mass conservation implies that the normal velocity  $V \sim k^{-\frac{1}{2}}h^2\beta^2$ , and then the streamwise momentum balance indicates that  $U \sim k^{-\frac{3}{2}}h^2\beta^2$ . This therefore yields the shear effect in (6.3c). So significant interaction can occur at low amplitudes ( $h$ ) in either of the two cases

$$\beta \sim h, k \sim h^2, h \ll 1 \text{ [Type c]}, \quad (6.4)$$

$$\beta \sim 1, k \sim h^2, h \ll 1 \text{ [Type d]}. \quad (6.5)$$

Other special cases cannot be discounted but the Types c,d appear to be substantial ones. The former, Type c, is summarized first below.

Type c's double structure (with  $Y \sim 1$  and  $Y \sim h^{-1}$ ) and its solution expansions proceed as guided by (6.4) and by comparison with Smith (1988b) and Hall and Smith (1989). The nonlinear interaction produced is found after some working to be governed by the induced-vortex equations

$$V_{\bar{Y}} + W_{\bar{z}} = 0, \quad (6.6a)$$

$$U_{\bar{t}} + V = U_{\bar{Y}\bar{Y}}, \quad (6.6b)$$

$$W_{\bar{t}} + \partial_{\bar{z}}(|\bar{P}|^2)\bar{Y}^{-2} = W_{\bar{Y}\bar{Y}} \quad (6.6c)$$

subject to

$$U_{\bar{Y}} \rightarrow 0, W \rightarrow 0 \text{ as } \bar{Y} \rightarrow \infty, \quad (6.6d)$$

$$U \sim \lambda_3 \bar{Y}, V \rightarrow 0, W \rightarrow \partial_{\bar{z}}(|\bar{P}|^2)\{-\ell n \bar{Y} + \phi\} \text{ as } \bar{Y} \rightarrow 0^+, \quad (6.6e)$$

coupled with the TS-wave equation

$$\bar{A}_{\bar{t}} = \{c_1 + c_3(\lambda_3^+ + \lambda_3^-)\}\bar{A} + c_4 \bar{A}_{\bar{z}\bar{z}} + c_5 \bar{A}|\bar{A}|^2 \quad (6.6f)$$

for  $\bar{A}(\bar{z}, \bar{t})$ . Here the coefficients in (6.6e,f) can be deduced from Sections 2-4 and Hall and Smith (1984),  $\bar{P}^+ - \bar{P}^- = -\alpha^2 I \bar{A}$  from (6.2e), and the scalings behind this interaction are given by

$$\partial_T \rightarrow \partial_T + h^2 \partial_{\bar{t}}, \partial_Z \rightarrow h \partial_{\bar{z}}, \quad (6.7a)$$

$$(P, A) = (\bar{P}, \bar{A}) \exp(i\alpha X - i\Omega T) + \text{c.c. [wave]}, \quad (6.7b)$$

$$(U, V, W) \rightarrow (h^{-1}\bar{Y} + hU, h^3V, h^3W), Y = h^{-1}\bar{Y} \text{ [vortex]}, \quad (6.7c)$$

while, again as before,  $\lambda_3(\bar{z}, \bar{t})$  denotes the correction to the skin friction. The equations (6.6a-e) apply at each wall ( $\pm$ ). Lower-order logarithmic terms involved in (6.7c) have no influence on the nonlinear interaction (6.6a-f). The solution properties would seem to be analogous to those in Smith (1988b) and Section 4, implying that Type c can act as a fore-runner to the full interactive-boundary-layer interaction (6.2a-e) or to Type d below.

The Type d nonlinear interaction in (6.5) is much stronger in the sense that it produces 0(1) effects, i.e., locally the mean flow is completely altered from the original PPF form, despite the smallness of the input TS wave amplitude  $h$ . Here again the details are largely as in Smith (1988b) (see also Hall and Smith, 1989), but modified for the temporal response, and we find in summary the nonlinear interactive system

$$V_{\bar{Y}} + W_Z = 0, \quad (6.8a)$$



$$U_{\bar{t}} + VU_{\bar{Y}} + WU_Z = U_{\bar{Y}\bar{Y}}, \quad (6.8b)$$

$$W_{\bar{t}} + VW_{\bar{Y}} + WW_Z = W_{\bar{Y}\bar{Y}}, \quad (6.8c)$$

with

$$U_{\bar{Y}} \rightarrow 1, W \rightarrow 0, \text{ as } \bar{Y} \rightarrow \infty, \quad (6.8d)$$

$$U \sim \lambda_v(Z, \bar{t})\bar{Y}, V \rightarrow 0, W \rightarrow -\lambda_v^{-2} \partial_Z \{|P|^2 + \alpha^{-2} P_Z P_Z^*\}, \text{ as } \bar{Y} \rightarrow 0+ \quad (6.8e)$$

for the vortex flow in the buffer zones, coupled with the TS-equation

$$P_{ZZ} - \lambda_v^{-1} \lambda_{vZ} \mathcal{F} P_Z - \alpha^2 P = \mp GA \quad (6.9a)$$

for the pressures  $P^\pm$  and displacements  $\propto \mp A$ , near either wall ( $\pm$ ). Here

$$\mathcal{F} = \frac{3}{2} + \frac{\xi_0 A i_0'}{2 A i_0'} \left[ 1 + \frac{\xi_0 \kappa}{A i_0'} \right], \quad (6.9b)$$

$$G = (i\alpha\lambda_v)^{\frac{5}{3}} \frac{A i_0'}{\kappa}, \xi_0 = -i^{\frac{1}{3}} \Omega (\alpha\lambda_v)^{-\frac{2}{3}}, \quad (6.9c, d)$$

and (6.2e) still relates  $P^\pm$  and  $A$ . Also, the scalings

$$Y = h^{-1} \bar{Y}, \partial_T \rightarrow \partial_T + h^2 \partial_{\bar{t}},$$

$$(P, A) \rightarrow h'(P, A)E + \text{c.c. [wave]}, \quad (6.10a - c)$$

$$(U, V, W) \rightarrow (h^{-1}U, hV, h^2W) \text{ [vortex]}$$

have been applied above, with  $h' \equiv h(-\ell nh)^{-\frac{1}{2}}$ , while the wave depends on  $T$  through the unknown frequency  $\Omega$  and wavenumber  $\alpha$  (both real) in  $E \equiv \exp(i\alpha X - i\Omega T)$  but the induced vortex motion is independent of the fast scale  $T$ . See further comments in Smith (1988b). The major solution properties here are still unknown, c.f. the last-named paper, although the weak linear case of secondary 3D instability for a 2D input TS wave can be established readily, and brings in Squire-mode destabilization, as in that paper, while a break-up singularity at finite time is a possibility in the full nonlinear system.

It is convenient now to reconsider the nonlinear interaction labelled Type b in Section 5. This arises as a distinct intermediate interaction between Types a,c. Thus, if the input amplitude  $h$  is reduced to order  $\epsilon$  in the Type c interaction then formally, from (6.4), the relative time dependence  $k$  slows to  $0(\epsilon^2)$ , the spanwise dependence  $\epsilon\beta$  reduces to  $0(\epsilon^2)$  and the outer buffer-zone extent  $\epsilon^2 h^{-1}$  increases to  $0(\epsilon)$ . These suggested scales tie in exactly with those inferred in Section 5 from the break-up of the Type a interaction. Thus, there is a match between a,b and between b,c. The special character of Type b is described already in Section 5 and here we add only that, unlike Type c, Type b has the vortex motion being forced both internally and through the wall conditions by the TS amplitude.

The final Type, e, to be considered needs only a brief mention, as it is the short-wave/long-vortex nonlinear interaction of Bennett, et al. (1988), consisting of a TS wave of time scale  $0(\epsilon^{-3})$  interacting with a vortex of the viscous time scale  $0(\epsilon^{-7})$ . Like Type d above, Type e is a very strong interaction in which the mean flow itself is one of the unknown quantities and is substantially changed from its original form. The main point of mentioning Type e here is that there is a match between it and Type d, in fact, since a reduction of the input amplitude  $h$  to order  $\epsilon^2$ , in Type d, increases the vortex time scale  $\epsilon^{-1}k^1$  to  $\epsilon^{-7}$ , in view of (6.5), and simultaneously increases the buffer extent  $y \sim \epsilon^2 h^{-1}$  to  $0(1)$ , so that the vortex flow occupies the entire channel. These and other features agree with the scalings for Type e.

Further connections exist between the various nonlinear interactions a-e, as shown schematically in Figure 9, e.g., a match of a with e is possible as noted in an earlier section. In addition, the early occurrence of each is dependent on the input amplitude ( $h$ ) and spanwise dependence or warping factor ( $\propto \beta$ ), whereas later occurrences of the interactions can happen either as by-passes or as the consequences of a break-up in an earlier occurring type, such as in Section 5 where Type b is set into action after the break-up of Type a.

## 7. FURTHER COMMENTS

As far as we are aware, the present theory is the first to show a mechanism for the formation of tongues, or their initiation, during channel-flow transition, starting from an input which is a near-2D TS wave. The mechanism involved in the Type a interaction say is highly interactive (see Sections 2-4), between the warped TS wave and its induced longitudinal vortex motion, and the interaction is found to be mutually reinforcing in the sense that the vortex flow and the warping of the TS wave amplify together very strongly. This is first through linear 3D secondary instability, but, beyond that, ultimately the nonlinear interaction leads to the vorticity-tongue formation as described in (g) in Section 4. Weaker warping can prevent the occurrence of such a tongue, we note, so that the present regime is in some respects a threshold one. The response for Type a seems quite dependent on the initial conditions even so and these could bring in extra, stronger, physical effects early on, i.e. a different structural start to the interaction could be made. One example of this is noted in Section 5, where Type a leads into Type b. Another is associated with the influence of a mean vortex motion  $[u^{(3)}, v^{(3)}]$ , or small cross-flow, present initially, which could alter the secondary instability properties of Section 4(b),(d) through the effects of the vortex's mean skin friction and momentum integral, for instance. In general, during the current stage for Type a, however, Figure 7 summarizes what happens physically as the tongue is initiated. The vortex becomes concentrated and accentuated first at a certain spanwise lo-

cation, along with the enhancement of the TS amplitude and phase there, compared with the earlier slightly warped TS wave with weak vortex motion. In the vorticity formation, the integrated momentum ( $\propto J$ ) of the induced vortex increases rapidly in magnitude, as does its skin-friction factors, leading to an increasingly significant impact on the mean streamwise momentum and wall shears of the total flow. Most of these theoretical features may tie in qualitatively at least with experimental and computational findings (see Section 1) on spanwise focussing and eventual formation.

Further studies indicated by the present work include the next regime in the tongue development (Section 5 and Figure 8), the effects of wall curvature, which may accentuate the vortex flow, the influence of the additional inflexional instabilities which the tongue behavior sets up, oblique TS waves and the application to boundary-layer transition (see Hall and Smith, 1988, 1989, and Smith, 1988b). The same comments apply also to Types b-e as well as to the 3D interactive-boundary-layer version in (6.2) which could be taken as a further Type, f. These interactions are of various strengths, the strongest being Types e,f. [Type c we note is equivalent to both cases I, II of Hall and Smith (1988c) and Type d corresponds to case III in the same paper.] There may be other significant types also. We tend to feel that it could be easy, and misleading perhaps, to miss many of the above types in purely computational work or crude theories. Further, it is possible that the present work may lead on eventually to provide insight into the structure of the so-called Lambda vortex and other stronger features of transitional flows.

## ACKNOWLEDGEMENT

The interest and comments of Dr. D. J. Doorly are gratefully acknowledged.

## References

- [1] Biringen, S., 1984, *J. Fluid Mech.*, **148**.
- [2] Biringen, S. and Maestrello, L., 1984, *Phys. Fluids*, **27**, 318.
- [3] Gilbert, N. and Kleiser, L., 1986, in *Direct and Large Eddy Simulation of Turbulence* (eds. U. Schumann and R. Friedrich), 1-18, Vieweg, Braunschweig.
- [4] Hall, P. and Smith, F. T., 1984, *Stud. in Applied Math.*, **70**, 91.
- [5] Hall, P. and Smith, F. T., 1987, ICASE Report No. 87-25, and *Proc. Roy. Soc.*, 1988, **A417**, 255-282.
- [6] Hall, P. and Smith, F. T., 1988, ICASE Report No. 88-46, and *Euro. J. Mechs.*, 1989, **B8**, 179-205.
- [7] Hall, P. and Smith, F. T., 1989, ICASE Report, to appear.
- [8] Herbert, T., 1984, AIAA Paper No. 84-0009.
- [9] Kleiser, L., 1982, *Lec. Notes in Physics*, **170**, 280-285, Springer.
- [10] Kleiser, L. and Laurien, E., 1985, AIAA Paper No. 85-0566.
- [11] Kozlov, V. V. and Ramazanov, M. P., 1982, Paper 4-82, ITAM, USSR, AN Novosibirsk.
- [12] Kozlov, V. V. and Ramazanov, M. P., 1983, *Izv. Akad. Nauk. SSSR, Mekh. Zhidk. i Gaza*, 43-47.
- [13] Kozlov, V. V. and Ramazanov, M. P., 1984, *J. Fluid Mech.*, **147**, 149-157.
- [14] Nishioka, M., Iida, S., and Ichikawa, Y., 1975, *J. Fluid Mech.*, **72**, 731-751.
- [15] Nishioka, M., Asai, M., and Iida, S., 1980, in *Lam.-Turbulent Transition* (eds. R. Eppler and H. Fasel), 37-46, Springer.
- [16] Nishioka, M. and Asai, M., 1985, in *Lam.-Turbulent Transition* (ed. V. V. Kozlov), 173-182, Springer-Verlag.
- [17] Orszag, S. A. and Kells, L. C., 1980, *J. Fluid Mech.*, **96**.
- [18] Orszag, S. A. and Patera, A. T., 1983, *J. Fluid Mech.*, **128**, 347-385.

- [19] Ramazanov, M. P., 1985, in Lam.-Turbulent Transition (ed. V. V. Kozlov), 184-190, Springer-Verlag.
- [20] Singer, B., Reed, H. L., and Ferziger, J. H., 1986, AIAA Paper No. 86-0433.
- [21] Smith, F. T., 1980, *Mathematika*, **26**, 187-210 and 211-223.
- [22] Smith, F. T., 1988a, *Computers and Fluids*, to appear. Presentation at R. T. Davis Memorial Symposium, Cincinnati, Ohio, June 1987.
- [23] Smith, F. T., 1988b, *Mathematika*, **35**, 256-273.
- [24] Bennett, J., Hall, P., and Smith, F. T., 1988, ICASE Report No. 88-45, submitted to J.F.M.
- [25] Zang, T. A. and Hussaini, M. Y., 1985, AIAA Paper No. 85-0296.
- [26] Zhou, H. and Wang, W. G., 1984, *Acta Mechanica Sinica*.
- [27] Smith, F. T., 1988b, ICASE Report No. 88-66; also Smith, F. T. and Walton, A. G., 1989, *Mathematika*, to appear.

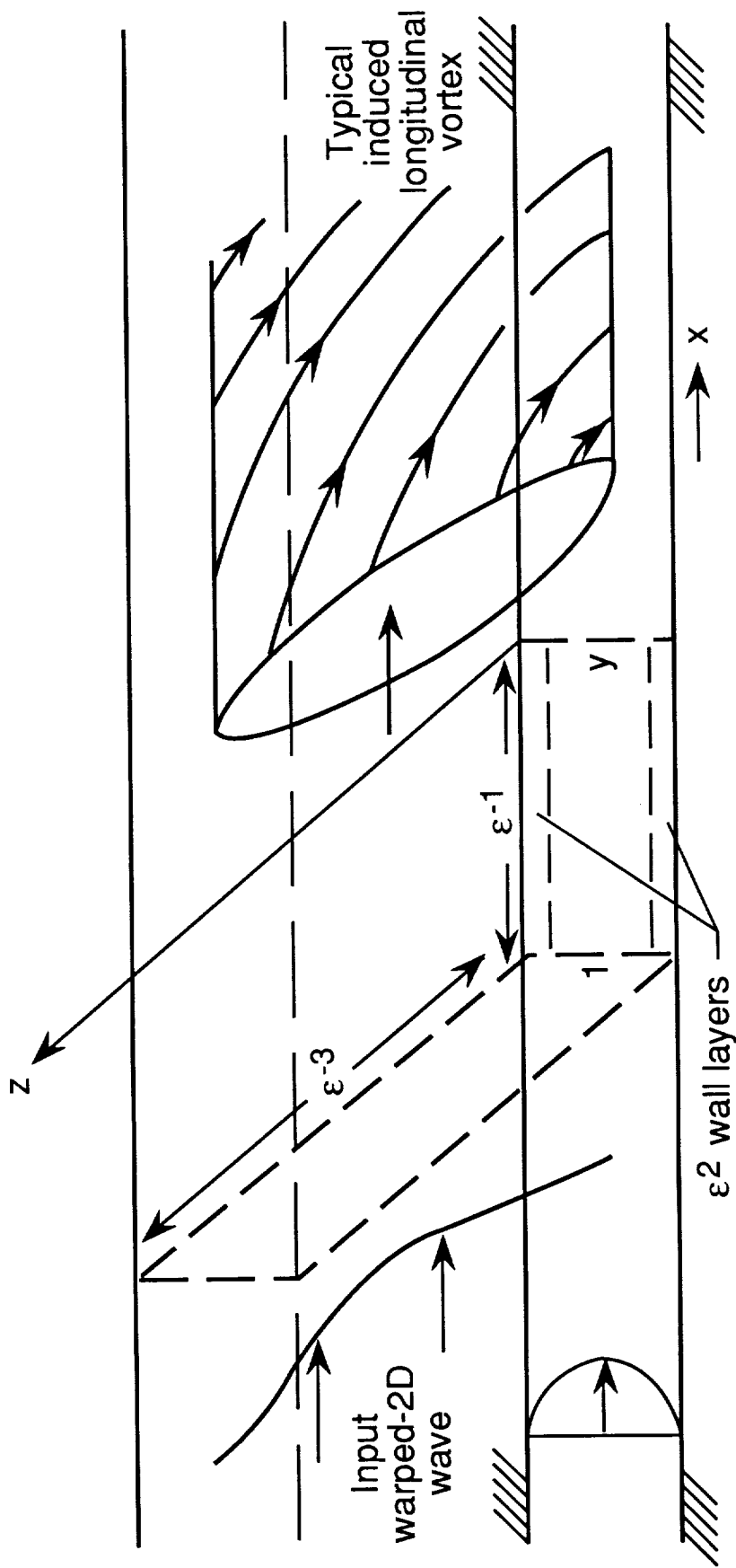


Figure 1.- The structure of the Type-a nonlinear interaction between a warped 2D TS wave and its induced longitudinal-vortex motion.

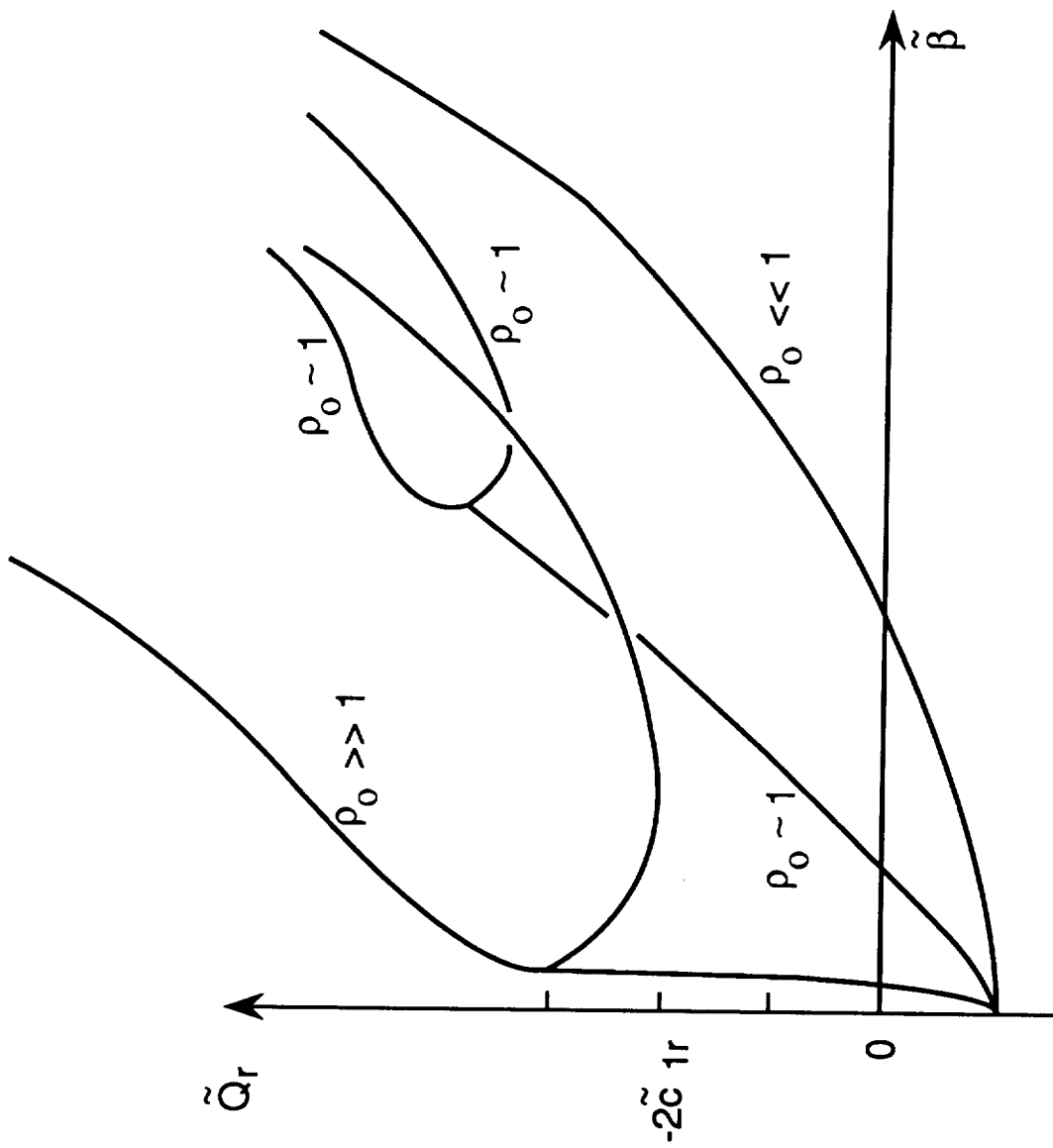


Figure 2.- The growth rate from (4.11c), when  $\tilde{c}_{1r}$  is negative.

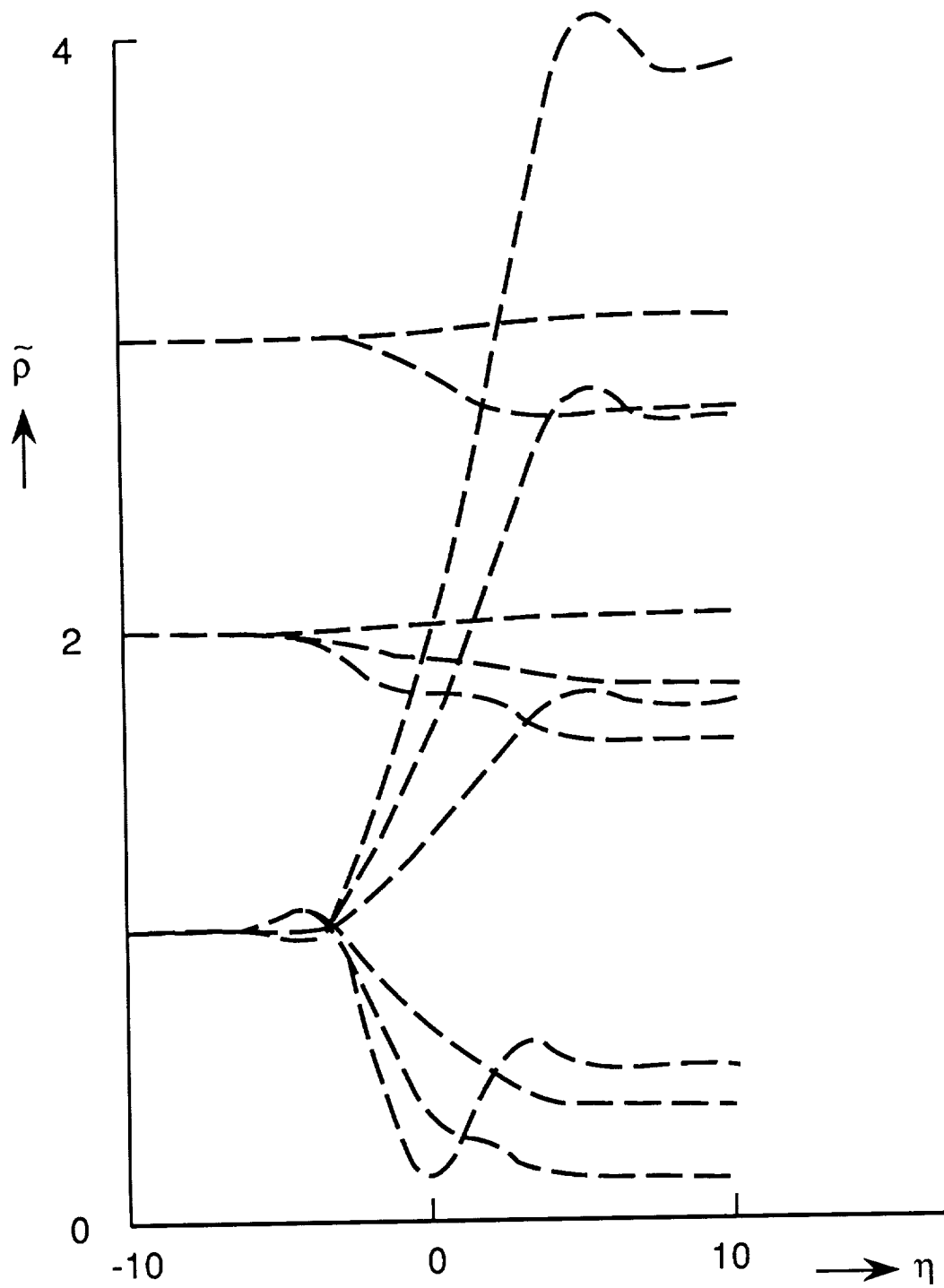


Figure 3.- Solutions of the shock-like terminal response (4.14a,b).



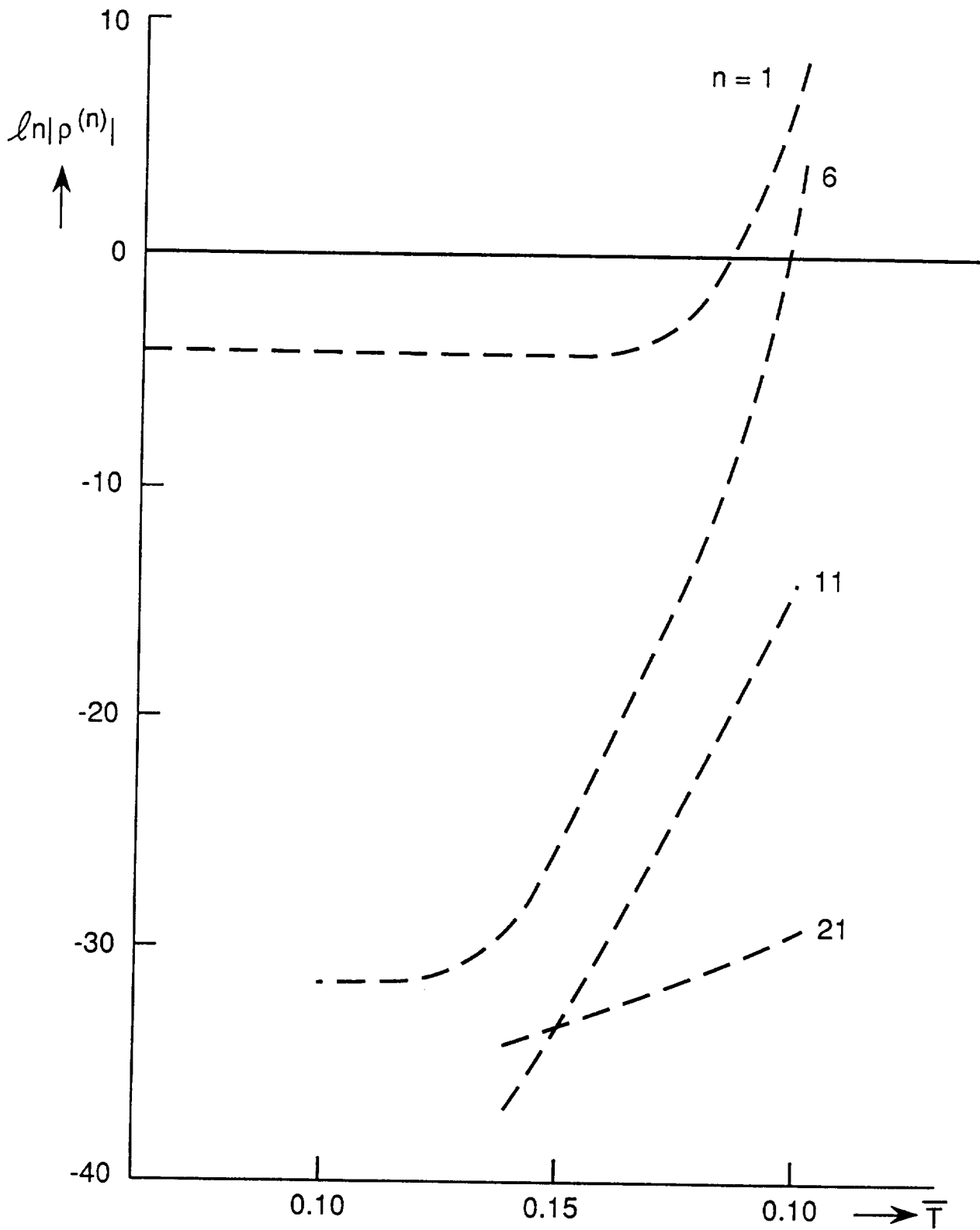


Figure 4.- Spectral solutions computed for (4.1a-e), (4.2): cf. Fig. 6. Time step  $\Delta\bar{T} = 0.0002$ ,  $y$ -step  $\Delta y = 0.05$ , truncation at  $M = 40$  terms. Initial condition  $v^{(3)}(n) = y^2(1 - y^2)$ ,  $\hat{A}^{(n)} = \exp\{-(n + 12)\}$ . Similar features resulted for other conditions and grids.

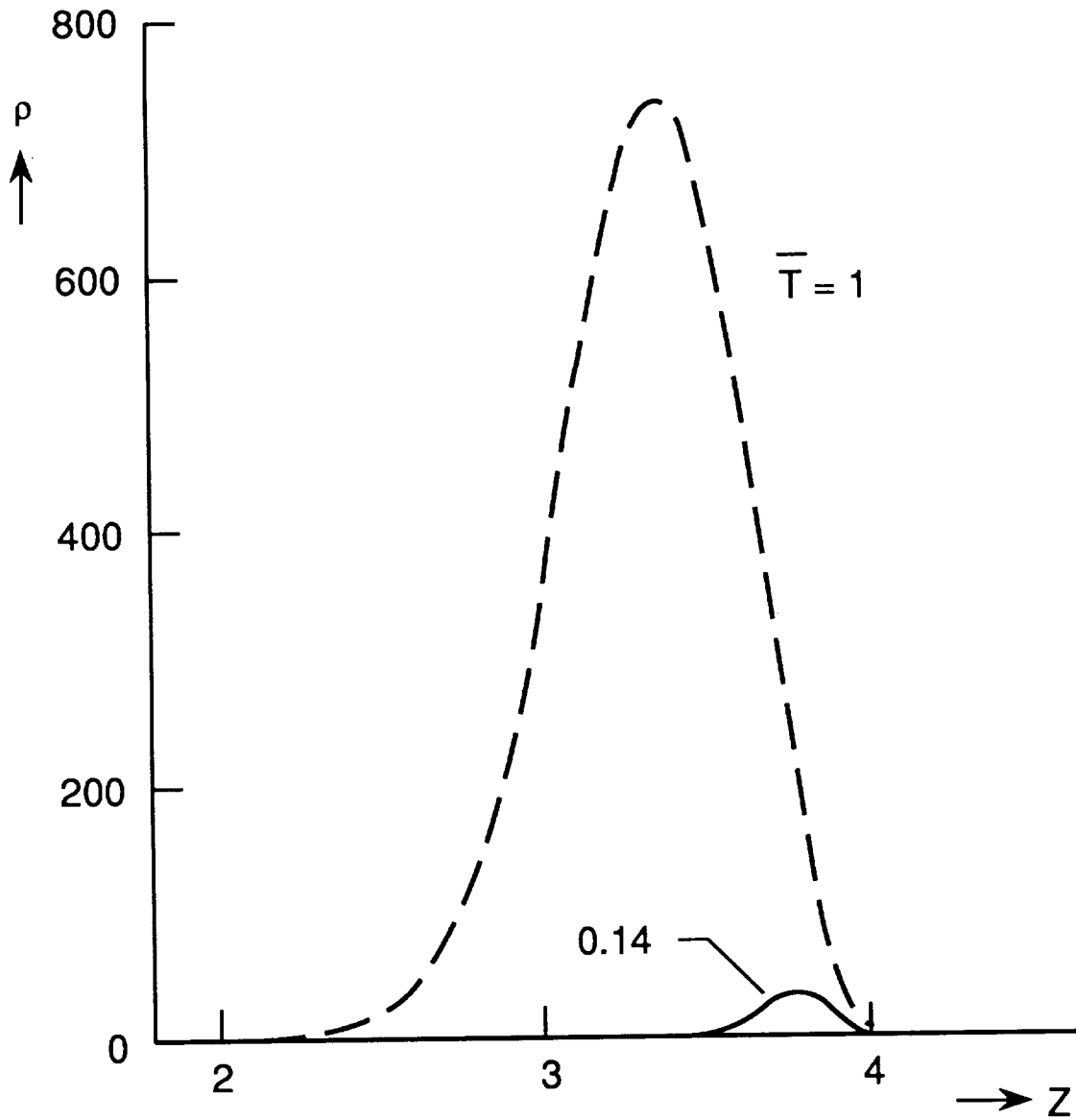


Figure 5.- Finite-difference computed solutions for (4.1a-e), (4.2). Here  $\Delta Z = 0.1$ ,  $\Delta y = 0.05$ ,  $\Delta \bar{T} = 0.001$ . Similar trends were found for other conditions used.

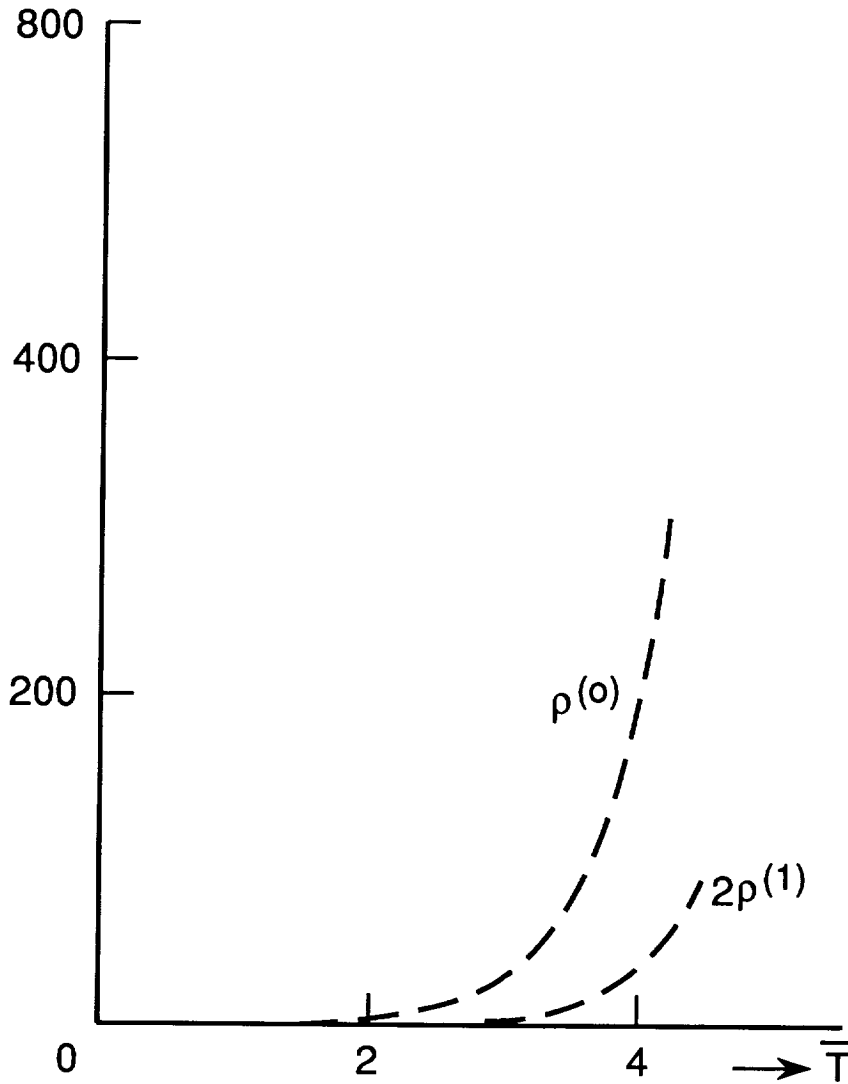


Figure 6.- Spectral solutions computed for (4.1a-e), (4.2) in the special case  $c_4 = 0$ . The representation  $\rho = \sum_0^{\infty} \rho^{(n)} \cos(n \pi Z/L)$  (etc.) with  $L = 2$  was truncated at  $M = 40$  terms. Here  $\Delta T = 0.0002$ ,  $\Delta y = 0.025$ ,  $C_1 = 0.9017 - 0.01189i$ . Initial condition:  $\hat{A}^{(n)} = \exp\{-(n+1)^2\}$ . Graphically identical results were obtained for  $(M, \Delta T, \Delta y) = (20, 0.0004, 0.05)$ . Vortex velocities  $u^{(3)}, v^{(3)}$  grow similarly in amplitude.

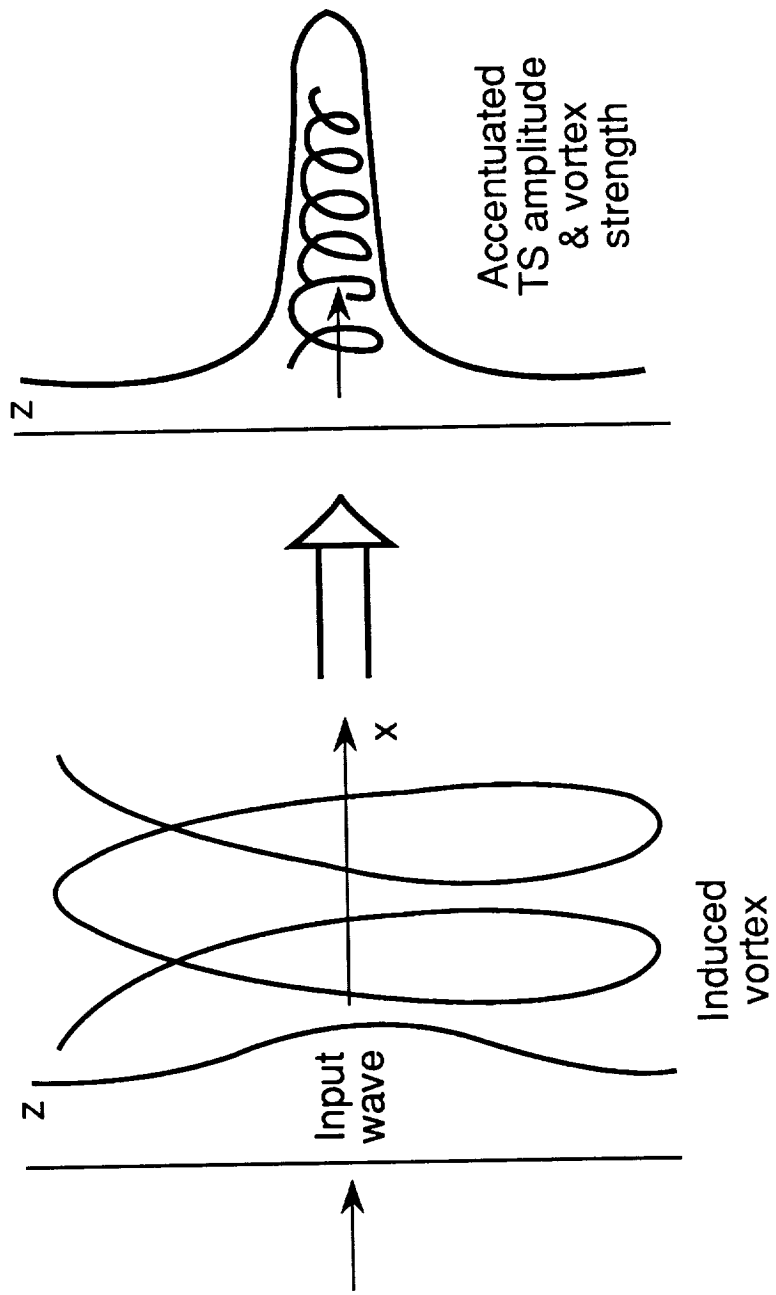


Figure 7.- Sketch of the streak-like breakdown: see (g) in section 4.

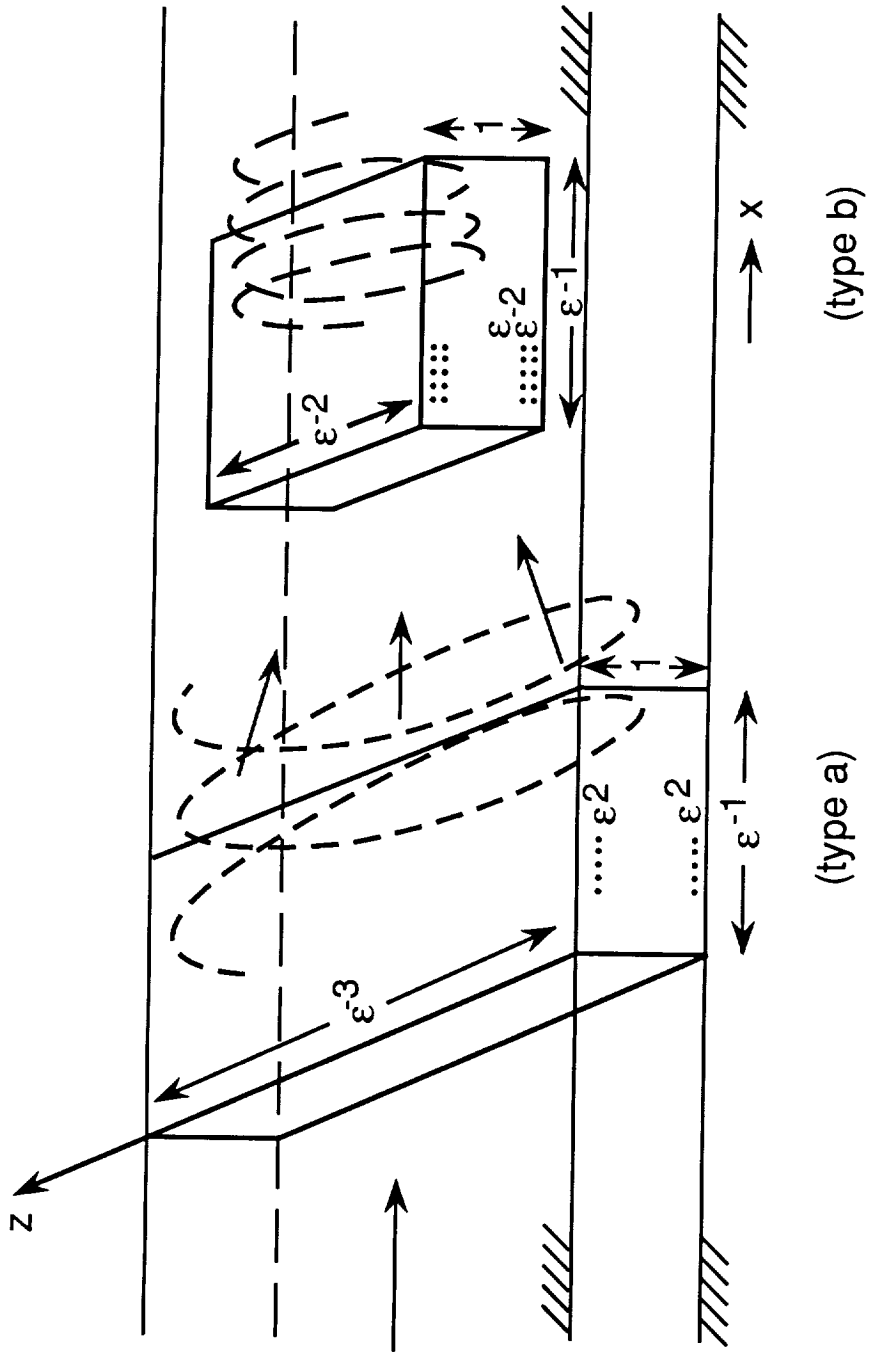


Figure 8.- The Type-b nonlinear interaction, spanwise focussed from Type a as shown. Similar focussing applies to the other types of interaction.

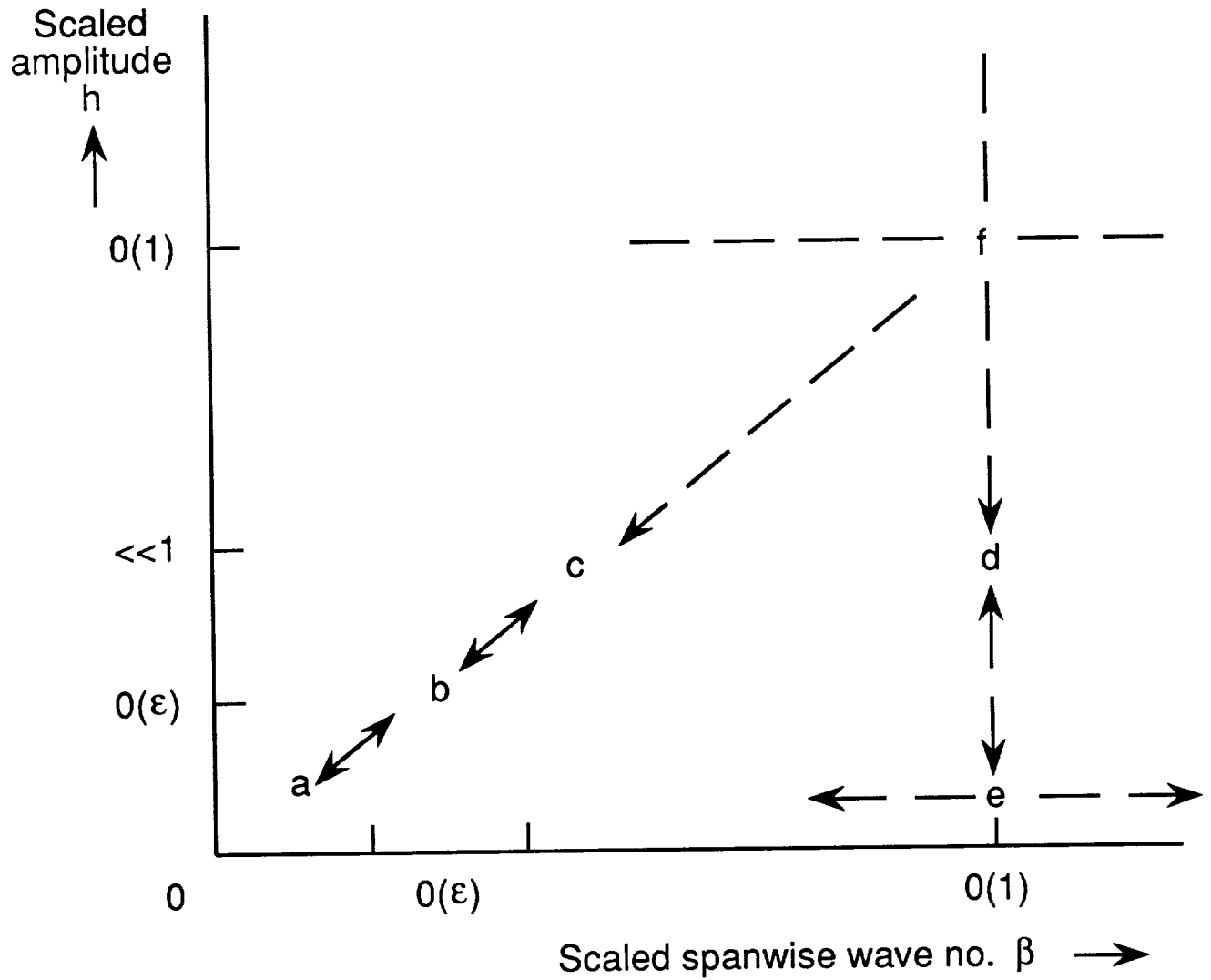


Figure 9.- Schematic diagram showing where the Types a-e of nonlinear interaction can occur, in the normalized amplitude-spanwise wavenumber  $(h-\beta)$  plane. Type f is the triple-deck-like case (6.2)



# Report Documentation Page

1. Report No. NASA CR-181928 ICASE Report No. 89-47		2. Government Accession No.		3. Recipient's Catalog No.	
4. Title and Subtitle  NEAR-PLANAR TS WAVES AND LONGITUDINAL VORTICES IN CHANNEL FLOW: NONLINEAR INTERACTION AND FOCUSING				5. Report Date September 1989	
				6. Performing Organization Code	
7. Author(s)  P. Hall F. T. Smith				8. Performing Organization Report No. 89-47	
				10. Work Unit No. 505-90-21-01	
9. Performing Organization Name and Address Institute for Computer Applications in Science and Engineering Mail Stop 132C, NASA Langley Research Center Hampton, VA 23665-5225				11. Contract or Grant No. NAS1-18605	
				13. Type of Report and Period Covered Contractor Report	
12. Sponsoring Agency Name and Address National Aeronautics and Space Administration Langley Research Center Hampton, VA 23665-5225				14. Sponsoring Agency Code	
				15. Supplementary Notes  Langley Technical Monitor: <span style="float: right;">Journal of Fluid Mechanics</span> Richard W. Barnwell  Final Report	
16. Abstract The nonlinear interaction between planar or near-planar Tollmien-Schlichting waves and longitudinal vortices, induced or input, is considered theoretically for channel flows at high Reynolds numbers. Several kinds of nonlinear interaction, dependent on the input amplitudes and wavenumbers or on previously occurring interactions, are found and inter-related. The first, Type a, is studied the most here and it usually produces spanwise focusing of both the wave and the vortex motion, within a finite scaled time, along with enhancement of both their amplitudes. This then points to the nonlinear interaction Type b where new interactive effects come into force to drive the wave and the vortex nonlinearly. Types c, d correspond to still higher amplitudes, with c being related to b, while d is connected with a larger-scale interaction e studied in an allied paper. Both c, d are subsets of the full three-dimensional triple-deck-like interaction, f. The strongest nonlinear interactions are those of d, e, f since they alter the mean-flow profile substantially, i. e., by an $O(1)$ relative amount. All the types of nonlinear interaction however can result in the formation of focussed responses in the sense of spanwise concentrations and/or amplifications of vorticity and wave amplitude.					
17. Key Words (Suggested by Author(s)) Tollmein-Schlichting Waves, longitudinal vortices			18. Distribution Statement 02 - Aerodynamics  Unclassified - Unlimited		
19. Security Classif. (of this report) Unclassified		20. Security Classif. (of this page) Unclassified		21. No. of pages 36	22. Price A03







